POLITECNICO MILANO 1863

SCHOOL OF INDUSTRIAL AND INFORMATION ENGINEERING

DEPARTMENT OF MECHANICAL ENGINEERING

Road Vehicle Stability under Crosswinds Using a Driving-Simulator-Calibrated Driver Controller

Tesi di Laurea Magistrale in Mobility Engineering

Flóra Budaházi

Student ID : 10969603

Supervisor: Prof. Gisella Tomasini

Co-supervisor: Eng. Carlos Esteban Araya Reyes

Academic year: 2025/2026

The research activities underlying this thesis were made possible thanks to the CROSS-STORM project funded by the European Union, NextGenerationEU, M4C2I1.1, Project PRIN 2022 PNRR "CROSS-STORM", Prot. 202284ZER9 – CUP D53D23003170006.

Funded by the European Union
NextGenerationEU

MUR Ministero dell'Università e della Ricerca

Italiadomani
PIANO NAZIONALE DI RIPRESA E RESILIENZA

Abstract in English

Adverse weather phenomena such as thunderstorms and downbursts generate non-synoptic wind conditions characterised by localised, high-intensity and rapidly varying gusts. Although these events pose a significant threat to road safety, most studies investigating wind–vehicle interaction focus on synoptic or moderate wind scenarios, leaving a gap in the assessment of vehicle stability under extreme, highly directional wind disturbances.

This thesis is part of the CROSS-STORM project that aims at developing a numerical-experimental procedure for evaluating the risk of a road accident due to crosswind generated by a thunderstorm. In particular the contribution of this thesis is to calibrate a driver controller using experimental tests and to analyse the influence of diverse parameters in the stability of the vehicle.

The study combines experimental and numerical approaches. Data collected from a driving simulator campaign were used to quantify vehicle response through selected risk indices describing lateral stability and load transfer. Based on these results, the vehicle control system was calibrated to ensure realistic dynamic behaviour. A systematic sensitivity analysis was then conducted to evaluate the influence of wind magnitude and direction across multiple operating conditions.

The outcomes of the analysis allowed the identification of relevant parameters influencing vehicle stability under crosswind conditions. The results showed that the risk level does not depend solely on wind intensity, but is also strongly affected by the vehicle trajectory and the dynamic interaction between driver and vehicle. A key outcome of this work is the validation and calibration of a driver controller capable of reliably reproducing vehicle behaviour under diverse wind and operating conditions. This validated simulation framework represents a consistent and robust tool for evaluating vehicle stability and crosswind response in different scenarios.

Keywords: Driving Simulator; Crosswind; Vehicle stability; Driver Controller

Abstract in Italian

Fenomeni meteorologici avversi come temporali e downburst generano condizioni di vento non sinottiche caratterizzate da raffiche localizzate, di elevata intensità e rapidamente variabili. Sebbene tali eventi rappresentino una minaccia significativa per la sicurezza stradale, la maggior parte degli studi sull'interazione vento–veicolo si concentra su scenari sinottici o su venti moderati, lasciando un vuoto nella valutazione della stabilità del veicolo in presenza di disturbi di vento estremi e fortemente direzionali.

La presente tesi si inserisce nel progetto CROSS-STORM, che mira a sviluppare una procedura numerico-sperimentale per la valutazione del rischio di incidente stradale dovuto a vento laterale generato da un temporale. In particolare, il contributo di questa tesi consiste nella calibrazione di un controllore del conducente mediante prove sperimentali e nell'analisi dell'influenza di diversi parametri sulla stabilità del veicolo.

Lo studio combina approcci sperimentali e numerici. I dati raccolti durante una campagna con simulatore di guida sono stati utilizzati per quantificare la risposta del veicolo attraverso indici di rischio selezionati, descrittivi della stabilità laterale e del trasferimento di carico. Sulla base di tali risultati, il sistema di controllo del veicolo è stato calibrato al fine di garantire un comportamento dinamico realistico. È stata quindi condotta un'analisi di sensibilità sistematica per valutare l'influenza dell'intensità e della direzione del vento in diverse condizioni operative.

I risultati dell'analisi hanno consentito di individuare parametri rilevanti che influenzano la stabilità del veicolo in condizioni di vento laterale. È emerso che il livello di rischio non dipende esclusivamente dall'intensità del vento, ma è fortemente influenzato anche dalla traiettoria del veicolo e dall'interazione dinamica tra conducente e veicolo. Un risultato fondamentale di questo lavoro è la validazione e calibrazione di un controllore del conducente in grado di riprodurre in modo affidabile il comportamento del veicolo in diverse condizioni di vento e di esercizio. Il framework di simulazione così validato rappresenta uno strumento coerente e robusto per la valutazione della stabilità del veicolo e della risposta al vento laterale in differenti scenari.

Parole chiave: Simulatore di guida; Vento laterale; Stabilità del veicolo; Controller del guidatore

Contents

List of Figures

List of Tables

01. Introduction

Extreme wind events represent a significant safety concern for road transportation systems. Crosswind disturbances can strongly affect vehicle lateral stability, trajectory tracking performance, and driver workload, especially in exposed infrastructures such as bridges, open highways, and tunnel exits [1, 2]. The interaction between aerodynamic loads, vehicle dynamics, and driver control actions becomes particularly critical when wind conditions vary rapidly in magnitude and direction [3].

Heavy vehicles are generally more sensitive to crosswind effects due to their larger lateral surface area and higher center of gravity. However, even passenger cars may experience substantial lateral displacement and steering corrections under strong wind conditions. Understanding these effects requires a combined analysis of aerodynamic disturbance modelling, vehicle dynamics response, and driver control behaviour.

Recent quantitative studies have provided increasingly precise estimates of how certain weather variables increase crash risk. For example, Becker (2022) analysed German crash data from 2006-2017 [4] using generalized additive models to estimate the effects of precipitation, temperature, sun glare, and wind, on different crash types and road and vehicle categories. They find that high wind speeds significantly increase the risk of certain types of crashes, especially single-truck crashes and 'hit object' crashes (where debris or objects are blown into the driving path). The study also uses the notion of 'relative risk increase (RRI)' to quantify how much worse the risk becomes under bad weather. The results reinforce the hypothesis that extreme wind events contribute non-negligibly to road safety risk, especially for heavy vehicles or when traffic speed and exposure are high.

Assessing the risk of accidents under extreme wind conditions is a complex task, requiring the integration of meteorological data, vehicle dynamics, and driver behaviour. Several methodologies have been proposed in the literature, ranging from statistical analyses to numerical simulations.

Early studies on wind-related accidents often relied on statistical methods, correlating historical crash data with meteorological conditions [4]. These approaches provide valuable insights into general trends and factors influencing accident likelihood, such as vehicle type, road geometry, and weather conditions. However, analytical models cannot predict the dynamics of individual events or quantify the impact of transient wind gusts on vehicle stability.

Semi-analytical models can be used to investigate vehicle stability and maximum safe speed. [5]

Recent studies increasingly employ numerical simulations to evaluate risk under realistic conditions. [6] These methods couple high-fidelity vehicle models with wind profiles and driver behaviour, enabling the estimation of accident risk indices for various combinations of vehicle types, speeds, and wind conditions. Simulations allow the creation of detailed risk maps, which can indicate the probability or severity of lane deviation, lane invasion, and rollover across a range of operational scenarios.

This work was developed within the framework of the CROSS-STORM project, which aims to investigate the impact of extreme crosswind events on road vehicles and to enhance safety assessment methodologies under adverse environmental conditions. In particular the contribution of this thesis is to calibrate a driver controller using experimental tests and to analyse the influence of diverse parameters in the stability of the vehicle.

The first phase of the study consisted of participating in and analysing a driving simulator campaign involving multiple vehicle configurations, namely a saloon car in part-load condition and a small lorry in both empty and laden configurations. The vehicles were tested along predefined trajectories under crosswind disturbances. In this context, driving simulators provide a safe and controlled environment to reproduce hazardous wind scenarios while ensuring repeatability of the experiments. The experimental campaign analysed in this thesis was conducted at the driving simulator facility of the Politecnico di Milano, known as DriSMi. The simulator enables the reproduction of wind disturbances acting on different vehicle configurations under controlled trajectory conditions. From the recorded experimental data, a set of risk indices was computed in order to quantify vehicle stability, trajectory deviation, and driver control effort.

The calculated risk indices served as a basis for retuning the PID controllers implemented in the vehicle model. The objective of the retuning process was to ensure that the simulated vehicle response better reflected the behaviour observed during the experimental campaign, while maintaining stability and realistic control performance.

Following controller calibration, a systematic sensitivity analysis was performed. Five wind velocity levels and nineteen wind direction angles were considered, generating a comprehensive set of wind scenarios. For each combination, the corresponding risk indices were evaluated, allowing the influence of wind magnitude and direction on vehicle behaviour to be quantified.

The contribution of this thesis lies in the integration of experimental driving simulator data, controller calibration, and systematic wind sensitivity analysis into a unified risk assessment framework. By combining experimental and simulation-based approaches, this work contributes to a deeper understanding of crosswind-induced vehicle instability and supports the objectives of the CROSS-STORM project in improving road safety under extreme weather conditions.

02. State of the Art

2.1. Wind modelling

Thunderstorms are localized events characterized by rapidly evolving air motions. They consist of convective cells where the air rises and sinks due to temperature differences, producing complex and transient wind patterns. A critical feature of thunderstorms is the downburst, a downdraft of cooled air that strikes the ground and spreads radially, generating intense horizontal gusts. These gusts can appear suddenly, with rapid increases in wind speed and abrupt changes in direction, creating significant hazards for vehicles, particularly high-sided or fast-moving ones [7].

Traditionally, wind modelling focused on synoptic or stationary wind fields, such as extra-tropical cyclones or steady gusts. Many early studies represented wind loads as either deterministic or quasi-steady, ignoring temporal variability and stochastic fluctuations. For example, Yu et al. (2019) [8] compared steady, gust, and turbulent wind models in the assessment of train crosswind stability, showing that steady wind models often simplify or underaccount for variability in dynamic responses under gust or turbulence conditions. While suitable for long-duration or spatially uniform flows, these stationary models fail to reproduce the transient, non-uniform nature of downbursts.

In recent years, the modelling of non-stationary and stochastic winds has gained attention, especially for applications in vehicle dynamics and structural safety. Hybrid methodologies combine deterministic representations of the mean flow, often based on analytical downburst or impinging jet models, with stochastic components that capture turbulence and random gust variations [9]. These approaches allow simulation of wind speed and direction as time-varying fields across multiple spatial points, providing more realistic inputs for vehicle aerodynamic and dynamics studies. Methods commonly used include Monte Carlo simulations, spectral decomposition of turbulence, and time-history reconstruction from analytical or measurement-based downburst profiles [10].

Overall, the evolution from stationary to stochastic, non-stationary wind models reflects the increasing recognition of the transient nature of thunderstorms and the need for accurate, dynamic assessment of vehicle safety under extreme weather conditions. In the framework of the CROSS-STORM project a methodology for defining the wind field experimented by a car traversing a downburst was previously developed. First, a semi-empirical model by Xhelaj et al [11]. is used to describe the main structure of the downburst, combining the radial outflow, the storm motion, and a background wind component. Then, realistic turbulence is added based on full-scale wind measurements, generating time-dependent wind fluctuations through Monte Carlo simulations. The mean wind and turbulence are combined to obtain the complete, time-varying wind field. Finally, the relative wind velocity acting on the moving vehicle is computed by considering its speed and direction as shown on Figure 2.1, providing the wind input for the aerodynamic and stability analyses.

2.2. Aerodynamics

Aerodynamic coefficients quantify the aerodynamic forces acting on a vehicle and are essential for evaluating its stability and performance un-

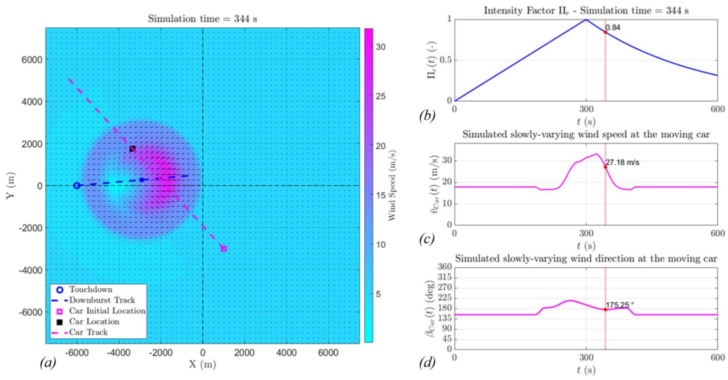

Figure 2.1: Trajectory of the vehicle and the downburst

der wind loads. These coefficients are typically determined through wind tunnel testing, which provides controlled conditions to measure the forces and moments acting on a model vehicle.

Historically, many studies have relied on computational fluid dynamics (CFD) simulations or simplified models to estimate aerodynamic coefficients. For instance, Rajkumar et al. (2003) [12] developed a neural network model optimized by a genetic algorithm to predict aerodynamic coefficients based on wind tunnel data. While such models can offer quick estimates, they may not capture the full complexity of real-world conditions, especially for non-stationary wind events like thunderstorms and downbursts.

In recent years, there has been a shift towards integrating CFD simulations with wind tunnel experiments to obtain more accurate aerodynamic coefficients. Liang et al. (2024) [13] employed a hybrid approach combining wind tunnel experiments and CFD simulations to analyse heavy-duty vehicle platoon aerodynamics, highlighting the importance of experimental validation in aerodynamic studies. Similarly, Zhang et al. (2024) [14] conducted wind tunnel tests to validate CFD simulations for a trains, demonstrating the necessity of experimental data for accurate aerodynamic modeling.

These advancements underscore the limitations of relying solely on CFD simulations or simplified models for determining aerodynamic coefficients.

Therefore, conducting dedicated wind tunnel tests is crucial for obtaining precise aerodynamic coefficients that accurately reflect the behaviour of the vehicle under various wind conditions.

2.3. Vehicle modelling

Accurate representation of vehicle dynamics is essential to evaluate the response to aerodynamic forces, particularly under extreme environmental conditions such as non-stationary winds. Several vehicle models exist, ranging from simple kinematic approximations to complex multibody simulations. The choice of model depends on the required balance between computational efficiency and fidelity.

The kinematic single-track model is the simplest representation of vehicle dynamics, focusing on lateral and yaw motions while neglecting tyre slip and longitudinal dynamics. It is widely used for trajectory planning and basic stability analysis due to its low computational cost. However, it cannot capture complex vehicle responses to transient aerodynamic forces.

Between the single-track model and full multibody simulations, a four-wheel model offers a moderate level of complexity. This approach models each wheel separately, allowing the simulation of longitudinal, lateral, and yaw dynamics in more detail. It provides an improved description of vehicle stability and load transfer compared to single-track models but does not fully account for suspension, body roll, or intricate component interactions. Studies using four-wheel models have shown better predictions of lateral behaviour during manoeuvres than single-track models. For example, Brandt et al. (2021) [15] applied a four-wheel vehicle model alongside a single-track model and a multibody model, to analyse high-speed stability under crosswinds, highlighting the improved representation of aerodynamic and dynamic effects. Nevertheless, four-wheel models remain insufficient for the precise assessment of vehicle response to extreme or non-stationary wind events.

Multibody dynamics (MBD) models represent the vehicle as a system of interconnected rigid bodies, including the body, suspensions, wheels, and steering components. This allows simulation of roll, pitch, yaw, and all relevant interactions between subsystems. Multibody models are capable of capturing complex dynamic events, such as vehicle response to gusty winds or sudden downbursts, which simpler models cannot reliably represent. Studies employing 14–18 degree-of-freedom multibody models have demonstrated the superior accuracy of these models for handling, stability, and rollover risk assessment [6, 14, 16].

Simpler models, such as single-track and four-wheel models are suitable for preliminary analyses, path planning, or low-complexity stability assessments. However, they cannot fully capture the complex interactions induced by non-stationary or stochastic wind fields. Therefore, multibody simulations, validated against experimental data, are essential for accurate evaluation of vehicle behaviour under extreme wind conditions. This justifies the use of a detailed 14 DOF multibody model within the CROSS-STORM project, which will be further explained in Chapter 2.5.

2.4. Driver behaviour modelling

Driver response plays a critical role in vehicle stability under crosswinds, acting as a feedback mechanism that counteracts disturbances. Some papers even researched the effect of driver's steering input based on the drivers' skills showing the importance on driver behaviour modelling [17]. Various approaches exist to model this behaviour, ranging from simple proportional-integral-derivative (PID) controllers to more advanced strategies [18, 19].

PID controllers are the most widely used approach to approximate human driver behaviour. They combine proportional, integral, and derivative actions to minimise the deviation from the intended trajectory, typically using steering angle or torque as the control input. PID-based driver models are popular because of their simplicity, intuitive tuning, and ability to capture general corrective behaviour in both steady and transient conditions. In the context of crosswinds, PID controllers can represent how a driver reacts to sudden gusts or non-stationary wind patterns by adjusting steering inputs in real time. Studies have shown that, while PID models cannot fully capture adaptive or anticipatory human behaviour, they provide a sufficiently accurate approximation for many vehicle stability analyses [3].

More sophisticated approaches, such as linear-quadratic regulators (LQR) and model predictive control (MPC), have also been applied to driver modelling. LQR optimises a cost function balancing tracking error and control effort, while MPC predicts future vehicle states to optimise steering inputs under constraints. These methods can better simulate idealised or constrained driver behaviour but are computationally expensive and less straightforward to tune [18].

Driving simulators provide a safe and repeatable environment to validate driver models. Experiments have been conducted to investigate driver lane-keeping under crosswinds, the effects of gusty wind on control inputs, and interactions with complex road geometries. The DiM-400 dynamic driving simulator at Politecnico di Milano allows high-fidelity reproduction of accelerations, visual, auditory, and haptic cues, as well as precise measurement of steering actions through a dynamometric steering wheel. This enables accurate evaluation and retuning of PID controllers based on real human responses to extreme wind conditions [20].

For the sake of the CROSS-STORM project a PID controller was selected. Driving simulator experiments are essential for validating and adjusting the PID controller, ensuring realistic reproduction of human corrective actions under strong crosswinds.

2.5. CROSS-STORM project

In order to characterise the aerodynamic behaviour of road vehicles under crosswind conditions, a comprehensive wind tunnel experimental campaign was carried out in a previous phase of this research project. The main objective of that campaign was to obtain reliable aerodynamic coefficients to be later used as inputs for vehicle dynamics simulations under variable wind conditions. The work described in this section was not performed by the present author, but constitutes the experimental foundation upon which the current study is built.

2.5.1. Aerodynamic characterisation of road vehicles through wind tunnel tests

The experimental tests were conducted at the Politecnico di Milano Wind Tunnel (GVPM) [21], a closed-circuit wind tunnel arranged in a vertical layout, featuring two test sections located on opposite sides of the loop. The tests relevant to this project were carried out in the low-turbulence test section, the lower part in Figure 2.2 , which is specifically designed for high-quality aerodynamic measurements. This section is characterised by low turbulence intensity, minimal mean velocity variations, and a maximum wind speed of 55 m/s. A rotating turntable installed in the test section allowed controlled variation of wind incidence angle relative to the vehicle models.

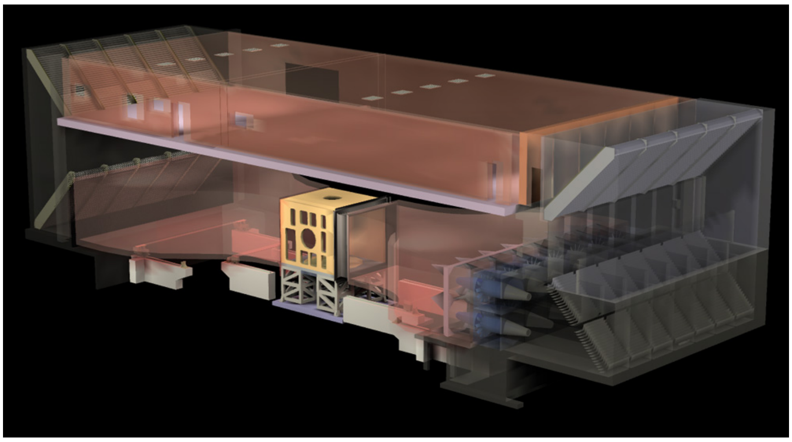

Figure 2.2: Wind tunnel facility

The experimental campaign included four vehicle types representative of the current road vehicle fleet: a Saloon Car, a Small Lorry, a Double-Decker Coach, and an Articulated Lorry shown on Figure 2.3. All models were rigid, meaning that only geometric characteristics were represented, while inertial, stiffness, and damping properties were not considered.

Consequently, the tests focused exclusively on aerodynamic load generation, without accounting for dynamic vehicle–wind interaction.

Figure 2.3: The tested vehicle models

The Saloon Car geometry corresponded to the well-known DrivAer model [22–24] shown in Figure 2.4, a generic yet realistic representation derived from typical mid-size passenger vehicles, mainly the Audi A4 and the BMW 3 series. This model is considered a benchmark case and has been used in several previous investigations [25–29]. A scaled model with a 1:4 ratio was used to ensure compatibility with the wind tunnel dimensions.

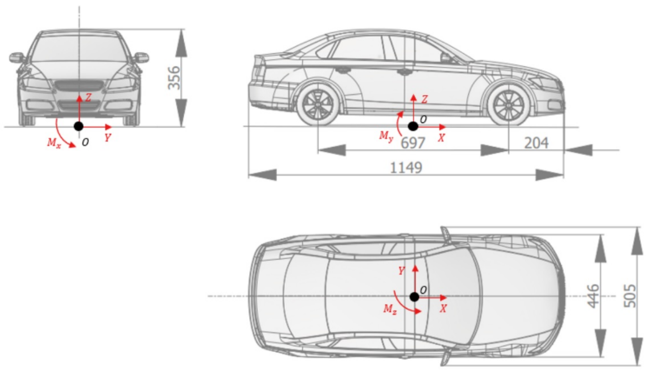

Figure 2.4: Main dimensions of Saloon car

The Small Lorry model was based on a Leyland DAF 45-130 van and was selected both for its representativeness and for the availability of previous experimental data [30–32], which enabled validation of the results. The main dimensions of the vehicle are shown in Figure 2.5. The Double-Decker Coach and the Articulated Lorry were included to capture the aerodynamic behaviour of large, high-sided vehicles, which are known to be particularly sensitive to crosswind effects.

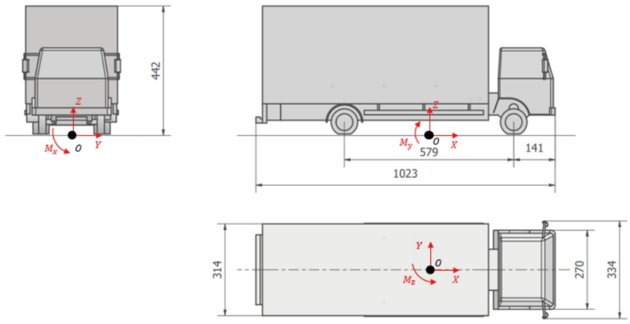

Figure 2.5: Main dimensions of Small lorry

All tests were performed under flat-ground conditions, representing vehicles travelling on open and level terrain. The models were mounted on a rotating platform, allowing wind incidence angles to be varied from 0° to 360° in 5° increments. Measurements were taken at wind speeds of 30 m/s and 50 m/s, except in cases where excessive vibrations limited the maximum yaw angle at higher speeds.

The measured aerodynamic forces and moments were converted into non-dimensional aerodynamic coefficients using standard formulations based on air density, wind speed, reference area, and reference height. In order to allow direct comparison across vehicle types, all aerodynamic coefficients were normalised using the same reference dimensions.

The experimental results showed that, despite differences in magnitude, the aerodynamic coefficients of all tested vehicles followed broadly similar trends as a function of wind incidence angle. The longitudinal force coefficient generally transitioned from negative to positive values as the yaw angle increased, indicating a shift from drag-dominated to thrust-assisting behaviour. The lateral force and roll moment coefficients exhibited closely correlated trends, suggesting that the height of the aerodynamic force application point remained approximately constant over a wide range of yaw angles.

The vertical force coefficient was predominantly positive, indicating the presence of lift, although exceptions were observed for certain vehicles and wind angles. The pitch moment coefficient was influenced mainly by the longitudinal force at small yaw angles and by the vertical force at larger angles. The yaw moment coefficient provided insight into the longitudinal position of the resultant aerodynamic force relative to the vehicle's centre of gravity.

While all four vehicle types were analysed in detail, particular attention was given to the Small Lorry and the Saloon Car, as these vehicles were selected for subsequent simulation-based investigations. The results showed that the Small Lorry exhibited significantly higher lateral force and roll moment coefficients than the Saloon Car, indicating a greater susceptibility to both lane deviation and rollover under crosswind conditions. This was further supported by the higher ratio between roll moment and lateral force, which is commonly used as an indicator of rollover risk.

In contrast, the Saloon Car displayed lower aerodynamic coefficients overall, primarily due to its smaller dimensions and more streamlined geometry. However, abrupt changes in several coefficients were observed at specific yaw angle ranges, associated with changes in flow behaviour and Reynolds number effects. These findings highlighted that, despite lower aerodynamic loads, passenger cars are not immune to crosswind-induced stability issues, particularly in terms of lateral displacement.

The wind tunnel campaign described above provides a validated and consistent set of aerodynamic coefficients for different vehicle categories under crosswind conditions. These coefficients constitute the baseline aerodynamic input data for the present thesis. In particular, the results obtained for the Small Lorry and the Saloon Car are directly relevant, as these vehicle types were selected for further investigation using co-simulation and vehicle dynamics models.

By building upon this prior experimental work, the present study focuses on analysing the dynamic response of vehicles subjected to crosswind, rather than on aerodynamic coefficient identification. The experimental campaign therefore represents a crucial preliminary step, ensuring that the aerodynamic inputs used in the subsequent simulations are physically meaningful and experimentally validated.

2.5.2. Multibody Simulation

To perform the dynamic simulations required for this study, a high-fidelity multibody vehicle model implemented in VI-CarRealTime (VI-Grade) was employed. VI-CarRealTime is a real-time vehicle dynamics simulation environment that enables off-line co-simulation with MATLAB/Simulink. The platform is widely used for advanced vehicle dynamics analyses and supports detailed modelling of passenger cars and commercial vehicles.

The vehicles are represented using a 14-degree-of-freedom (DOF) model [33] as shown in Figure 2.6. Six DOFs describe the motion of the vehicle body (longitudinal, lateral, and vertical translations, together with roll, pitch, and yaw rotations), while the remaining eight DOFs correspond to the vertical displacement and rotational speed of each tyre. The equations of motion are symbolically derived and parametrised within the software environment. Tyre forces are computed using the Pacejka tyre model [34], ensuring a realistic representation of tyre-road interaction.

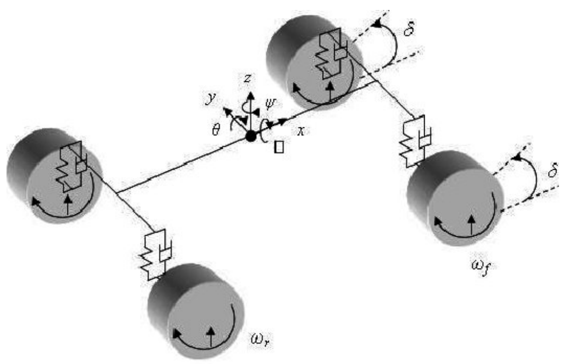

Figure 2.6: Schematic representation of 14 DOF vehicle model

The suspension and steering systems are modelled using simplified representations based on look-up tables. Instead of explicitly modelling physical components such as linkages, bushings, or steering racks, the kinematic and compliance characteristics are defined through parameterised datasets. The brake and powertrain subsystems are described using differential and algebraic equations. This modelling approach allows accurate dynamic behaviour while maintaining computational efficiency suitable for co-simulation.

The aerodynamic forces and moments are not natively integrated within the VI-CarRealTime environment. In the simulation framework adopted for this project, aerodynamic loads are calculated externally in MATLAB/Simulink and applied to the multibody model during co-simulation. The detailed formulation and implementation of the aerodynamic load calculation were developed in prior work [35] and are not reproduced here; only the aspects relevant to the present study are considered.

The Saloon Car model used in this work is based on the DrivAer multibody model available in VI-CarRealTime. The vehicle was considered in three mass configurations, which are the following: empty, part-load, and laden.

The heavier and lighter variants were generated by modifying the total vehicle mass while preserving the main dynamic characteristics of the baseline model. The total mass difference between the empty and laden configurations is approximately 700 kg.

For these configurations, the centre of gravity (CG) position is assumed to remain unchanged, as its variation due to loading is considered negligible for the purposes of this study.

Similarly, empty, part-load and laden mass configurations of the Small Lorry were considered.

In this case, the Empty and Laden configurations were available from previous research, while the part-load variant was derived as an intermediate case. Since its mass lies midway between the empty and laden configurations, both the CG location and the principal moments of inertia were obtained by interpolating between the corresponding values of the two reference configurations.

Unlike the Saloon Car, the variation in CG position for the Small Lorry was considered significant and therefore explicitly accounted for in the model definition.

The Small Lorry features a dual rear-wheel configuration (four wheels on the rear axle). The naming convention adopted for the wheels is consistent with that used in the result plots presented in the following chapters.

2.5.3. Risk indices

In order to compare cases under different operating conditions and to identify the most critical scenarios, three risk indices have been adopted. These indices are based on the lateral displacement of the vehicle and on the load transfer between the left and right sides. These indices were defined previously during the CROSS-STORM project and have been already used for other evaluations.

The first index is the Lateral Deviation (LD), which quantifies the lateral displacement of the vehicle from the ideal reference path. It is measured in meters and calculated in the vehicle reference frame. The critical threshold defined for this index varies by vehicle type as it is influenced by the width of the vehicle, it corresponds to 1 m in case of the saloon car, and to 0.625 m for the lorry.

$$LD = y_{vehicle} - y_{reference} \tag{2.1}$$

The second index is the Lane Invasion Index (LI). This index provides a direct measure of the remaining available space between the vehicle and the edge of the lane. It is expressed as a percentage and is considered critical when it becomes smaller than 0%, indicating that the vehicle is already invading the adjacent lane. The lane width has been fixed at 3.75 m, in accordance with the Italian standard [36]. The vehicle width is defined as the overall width excluding the side mirrors and is equal to 1.78 m for the Saloon Car model and 2.5 m for the Small Lorry.

$$LI = \frac{\frac{Lane\ width - Vehicle\ width}{2} - |LD|}{\frac{Lane\ width - Vehicle\ width}{2}} \cdot 100 \tag{2.2}$$

The final index is related to the load transfer and is referred to as the Load Transfer Ratio (LTR). It quantifies the amount of vertical load transferred from one side of the vehicle to the other under the action of lateral forces and is commonly used to evaluate the potential risk of vehicle rollover. The index is expressed as a percentage and is considered critical when it exceeds 100%. The vertical forces acting on the left tyres and on the right tyres appear in the numerator. In the denominator, the corresponding static vertical forces are used. These forces are obtained under constant vehicle speed on a straight trajectory with no wind action.

$$LTR = \frac{F_{zLeft} - F_{zRight}}{F_{zLeft,static} - F_{zRight,static}} \cdot 100 \tag{2.3}$$

03. Driving Simulator Campaign

When executing the driver simulator campaign, the previously defined PI controller is replaced by a human driver, creating a Driver-in-the-Loop (DiL) configuration. This mode of simulation enables real-time interaction between the driver and the system through the driving simulator. The vehicle model carries out the inputs of the driver in real time, and the simulator responds instantly with visual, auditory, and physical feedback, replicating the experience of driving a real vehicle. The model must be sufficiently efficient to operate in real time, avoiding any delays that could compromise the immersion or realism of the simulation. VI-CarRealTime allows for this type of simulation, as it runs at a speed that exceeds real-time performance, depending on the computer platform [37].

3.1. Driving Simulator Setup

For structuring the driving simulator test, a sensitivity analysis was conducted with the multibody model in Simulink and VI-Car. The five main variable of these analysis were the following: vehicle velocity, vehicle weight, vehicle trajectory, wind velocity and wind direction. In case of the lorry the velocity ranges from 80 km/h through 90 km/h to 100 km/h. The saloon car has a higher speed range, including 100 km/h, 120 km/h and 130 km/h. Considering the weight both vehicle types were tested in empty, part-load and laden conditions. The corresponding values are shown in Table 3.1.

	Saloon car	Small lorry
Empty	1650 kg	5361 kg
Part-load	1986.62 kg	9180 kg
Laden	2200 kg	13000 kg

Table 3.1: Vehicle weight configurations

On Figure 3.1 the four trajectory cases are presented: one straight trajectory parallel to the X axis and three circular trajectories. The three turning trajectories start with an initial straight section of 700 m, followed by curves with a radius of 400 m, 500 m, and 800 m.

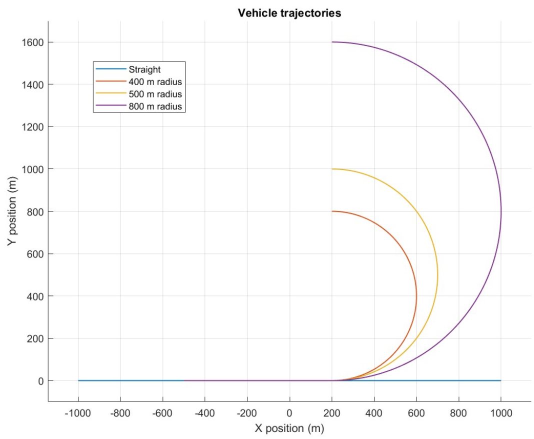

Figure 3.1: Trajectories defined for sensitivity analysis

The tested wind configurations correspond to the higher values on the Beaufort scale, from 7 to 11, mimicking gales and storms. Regarding the direction of the wind it was modified in 45 degree increments, resulting in eight possible directions in case of the curved trajectories. When the trajectory is straight the results would be symmetric therefore in that case only from 0° to 180° testcases were performed. In Table 3.2 all the wind magnitudes and directions are summarized.

Wind velocity	Wind angle
15 m/s	0°
20 m/s	45°
25 m/s	90°
30 m/s	135°
	180°
	225°
	270°
	315°

Table 3.2: Summary of wind configurations

The sensitivity analysis served as the basis for defining the scenarios implemented in the driving simulator campaign. The analysis allowed the identification of the parameters that most strongly influence vehicle stability, namely vehicle type, weight configuration, velocity, trajectory type.

A consistent difference between the two vehicle categories was observed. The Saloon Car showed significantly lower values of the selected risk indexes (Lateral Displacement and Load Transfer Ratio) for all tested combinations, always remaining below critical thresholds. On the other hand, the Small Lorry proved to be considerably more sensitive to wind disturbances and curved trajectories, exceeding critical limits in multiple cases. The most critical situations were associated with curved paths under increasing wind magnitude, and straight trajectories under cross-wind conditions at higher wind speeds. The analysis also showed that increasing vehicle mass mitigates the effect of wind, since a larger aerodynamic force is required to generate the same lateral displacement or load transfer.

3.2. Driving Simulator Facility

The driving simulator of Politecnico di Milano, referred to as DriSMi [38], allows virtual testing of different vehicle types within a fully controlled and safe environment. The repeatability of the experimental conditions ensures reliable and reproducible results, which are essential for quantitative analysis.

The simulator is built around a 6×6 m platform. Its main motion interface consists of a disk-frame system actuated by four cables operating over a 4×4 m horizontal area. The mechanical design decouples translational and rotational motions of the disk-frame, allowing more accurate and stable motion control.

The disk-frame moves across the platform by means of three air pads, which guarantee smooth sliding. In addition, a hexalift mechanism provides six degrees of freedom (6 DOF) to the cockpit, further increasing the fidelity of motion reproduction.

To enhance realism, the cockpit is equipped with eight on-board shakers that simulate vibrations generated by the engine and road surface irregularities. An active seatbelt system and an active seat reproduce the effects of longitudinal and lateral accelerations on the driver. Acoustic feedback is provided by a surround sound system composed of five internal speakers, capable of reproducing both interior and exterior noise sources. Visual immersion is achieved through a 270° projection screen that surrounds the driver and places them at the centre of the simulated environment.

Figure 3.2 shows a photograph taken during the experimental campaign, where the projected visuals contributed to reinforcing the perception of adverse weather conditions for the driver.

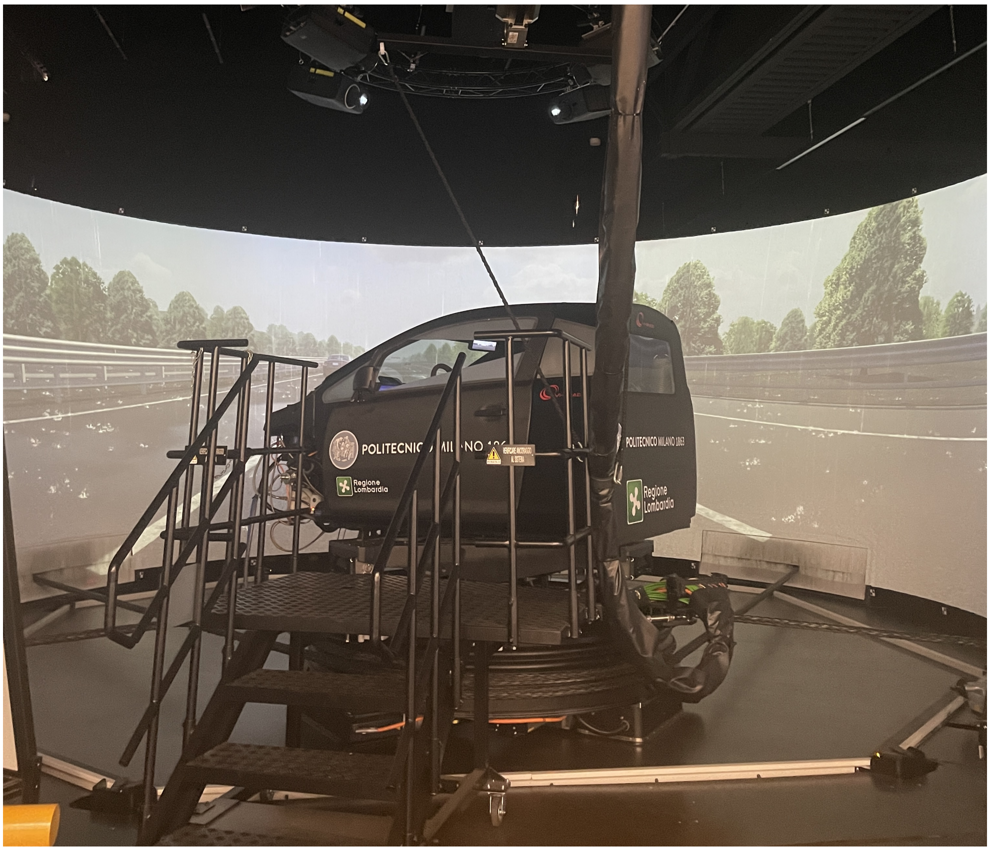

Figure 3.2: Driving simulator facility

3.3. Test scenarios

The experimental campaign involved two vehicle categories: a Saloon Car tested in Part-Load condition and a Small Lorry assessed in both Empty and Laden configurations. The inclusion of the two loading conditions for the Small Lorry was intended to capture the influence of mass variation on vehicle response under downburst wind excitation, whereas for the Saloon Car the Part-Load configuration was considered representative of typical operating conditions.

Two different trajectories were implemented in the driving simulator environment in order to account for both purely longitudinal and combined lateral–longitudinal vehicle dynamics. The first consisted of a straight trajectory with a total length of 2 km, while the second comprised a curved layout formed by an initial straight segment followed by a semi-circular section with a radius of 500 m. The trajectories are visually displayed on Figure 3.3.

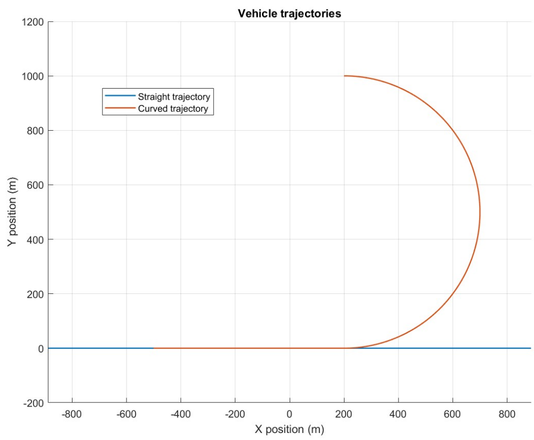

Figure 3.3: Trajectories defined for experimental campaign

On Figure 3.4 the tested scenarios are summarized, also indicating the the order in which the scenarios were executed from the left to the right.

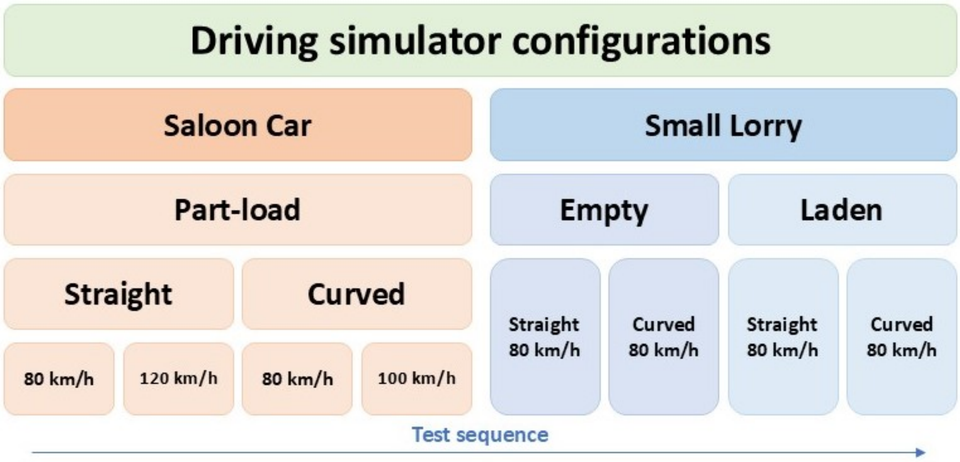

Figure 3.4: Driving simulator campaign configurations

For comparability purposes, all vehicle configurations were tested at a constant target speed of 80 km/h. This ensured a consistent basis for evaluating the differences between the Saloon Car and the Small Lorry, as well as between the Empty and Laden states of the latter. In addition to this reference speed, higher velocities were examined for the Saloon Car in order to reflect its typical operating range. Specifically, a target speed of 120 km/h was adopted for the straight trajectory, while a maximum speed of 100 km/h was imposed for the curved configuration, in line with conventional speed limits and representative driving conditions.

Although target velocities were predefined, no cruise control system was implemented. This choice was made intentionally to analyse potential spontaneous driver reactions under adverse wind conditions, particularly any instinctive reduction in speed due to a perceived loss of safety. While this approach may slightly reduce repeatability, it provides valuable insight into driver behaviour and adaptive responses under extreme atmospheric events. The drivers aim during the test were the control the vehicle's speed in the plus minus 5 range around the defined speed and to keep the vehicle in the lane. In the fifth scenario the empty lorry is not able to maintain the suggested speed due to lack of grip between the tyres and the road surface.

The virtual scenarios were developed using RoadRunner and VI-WorldSim, enabling co-simulation with VI-CarRealTime, Simulink, and the driving simulator platform.

For the experimental campaign, a realistic downburst wind time history was provided by the research team from University of Genoa. This team has been studying and successfully modelling downburst events [11, 39]. In order to ensure consistency and comparability among the different test cases, identical storm conditions were applied throughout all simulations. Nevertheless, the actual aerodynamic load experienced by each vehicle differed depending on its trajectory, travelling speed, and instantaneous position within the wind field.

The simulated downburst was characterised by a translational velocity of 10 m/s and peak wind speeds of approximately 30 m/s. An example of the resulting wind field for the straight trajectory configuration at 80 km/h and 120 km/h are presented in Figures 3.5 and 3.6, respectively.

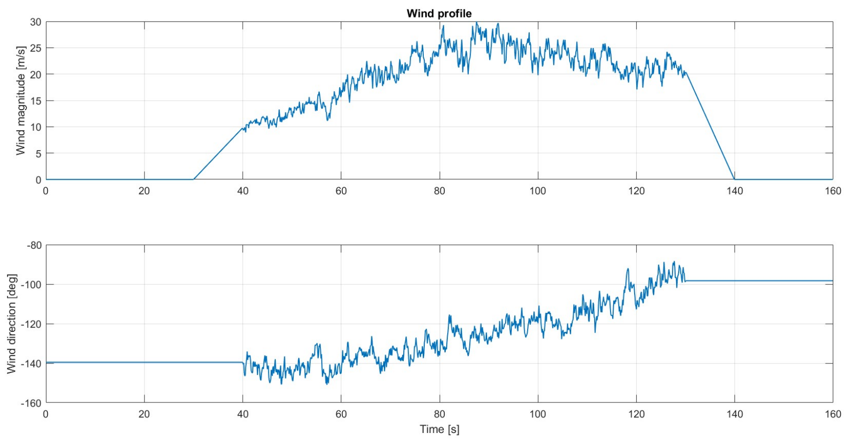

Figure 3.5: Wind profile applied in 80 km/h straight scenarios

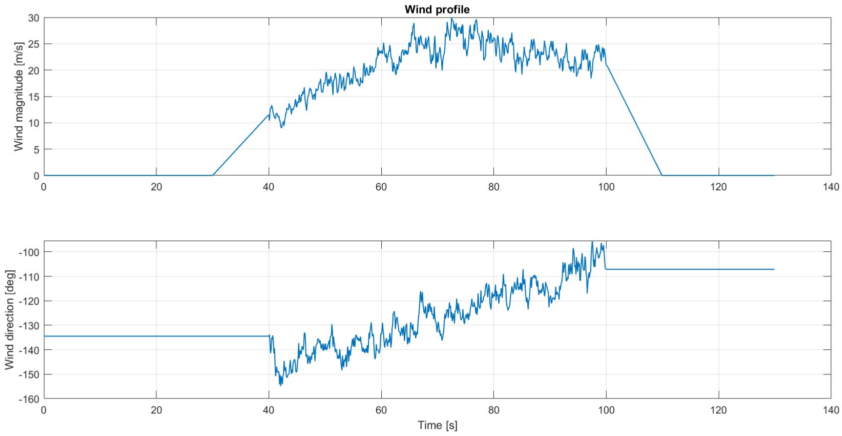

Figure 3.6: Wind profile applied in 120 km/h straight scenario

Overall, eight test conditions were defined. Depending on the specific trajectory and vehicle speed, each test lasted between approximately 100 and 150 seconds. Including preparation time and configuration changes, around 30 minutes were allocated per participant.

During the experiments, drivers were instructed to remain within their designated lane as consistently as possible and to maintain the prescribed target speed for each scenario. All participants followed the same test sequence. The campaign began with the Saloon Car model: first the straight trajectory at 80 km/h and 120 km/h, followed by the curved trajectory at 80 km/h and 100 km/h. The vehicle model was then switched to the Small Lorry Empty configuration, which was tested on both trajectories at 80 km/h. Finally, the Small Lorry Laden configuration was assessed following the same procedure.

3.4. Population, Test participants

A group of 43 drivers aged between 20 and 28 participated in the driving simulator experimental campaign. The relatively narrow age range was intentionally selected in order to limit variability associated with age-related factors, such as differences in driving experience or reaction times. By constraining the age distribution, age-related influences were minimised, allowing the PID controller tuning process to focus on vehicle dynamics and control performance rather than inter-driver variability.

All participants were students at Politecnico di Milano, resulting in a relatively homogeneous test population in terms of educational background and familiarity with technology. They possessed a valid driving licence, with prior real-world driving experience involving passenger cars. None of the participants had previous experience driving heavy-duty vehicles or lorries. While this choice limits the generalisability of the results to broader driver populations, it provides a consistent and controlled reference for the purposes of controller calibration and comparative analysis. Participation in the experimental campaign was voluntary and no financial compensation was provided.

The test population consisted of 11 female and 32 male drivers. While gender was not treated as an independent variable, both female and male participants were included in order to better approximate real-world driving conditions and to reduce the risk of tuning the controller based on a single driver demographic.

Future research could include additional simulator-based testing campaigns involving drivers from different age groups and experience levels in order to adapt the controller parameters to a wider range of driving behaviours and demographic characteristics.

3.5. Results

Figures in this section present the results obtained from the driving simulator campaign. Each driver is represented by a red dot on the figure, while the lines serve as describing the whole population. The thick black line indicates the median value of the data set, while the dashed blue line placed from plus and minus one standard deviation from the median. The four previously presented risk indices are showcased on the plots to evaluate the hazards in each scenario. On the top left corner the lateral deviation is reported, below that the corresponding lane invasion index, while on the right side respectively the front and rear load transfer ratios are displayed. In case of lateral deviation and load transfer the maximum value that occurred during the test is indicated, not considering if the vehicle diverges to the left or the right, and also if the load is shifted to the left or the right side of the vehicle. Since the lane invasion is inversely proportional, the minimum value of it is evaluated, therefore this is the only parameter that can reach negative values indicating that the vehicle has left the lane. The safety threshold for lateral deviation depends on the width of the vehicle, in case of the saloon car it is around 1 m, which corresponds to 0% in lane invasion. While for the lorry configurations it is around 0.6 m. The safety threshold for the load transfer ratio is 100%, but important to point out that a 100% or higher LTR does not necessary mean that the vehicle rolled over. The shown numbers are momentary values, for the vehicle to actually roll over momentarily unloading of one of the wheels is not enough.

On Figure 3.7 the performance distribution of the 43 drivers is presented at the first test scenario, which was conducted with the saloon car on a straight road at 80 km/h. We can confidently say that this was the safest scenario among the tested scenarios based on the drivers evaluation. This was also the first test for all the drivers so they had no prior experience driving on the simulator during this run. In case of the lateral displacement of the vehicle some drivers crossed the safety threshold, but the values are generally close to each other, mostly staying in the standard deviation range except for some outliers. The median is below the threshold of 1 m. The load transfer on both axles stayed quite low during all the test drives, never overcoming even the 25% value, but in most cases it stays below 15%.

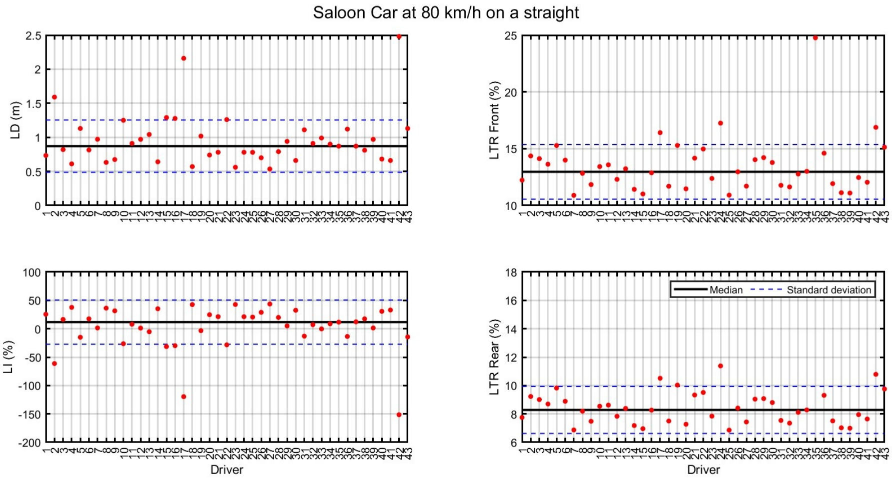

Figure 3.7: Performance distribution among drivers - Saloon Car at 80 km/h

On Figure 3.8 we can observe similar values in the 120 km/h scenario as in the previous 80 km/h scenario. The median of the lateral deviation is right on the 1 m threshold. The load transfer values are slightly higher than at lower speed, an around 5% increase can be detected. It is interesting to mention that even though by looking at the numbers this scenario rises no concerns regarding safety, in the post-drive evaluations the drivers selected this scenario as the third most dangerous one.

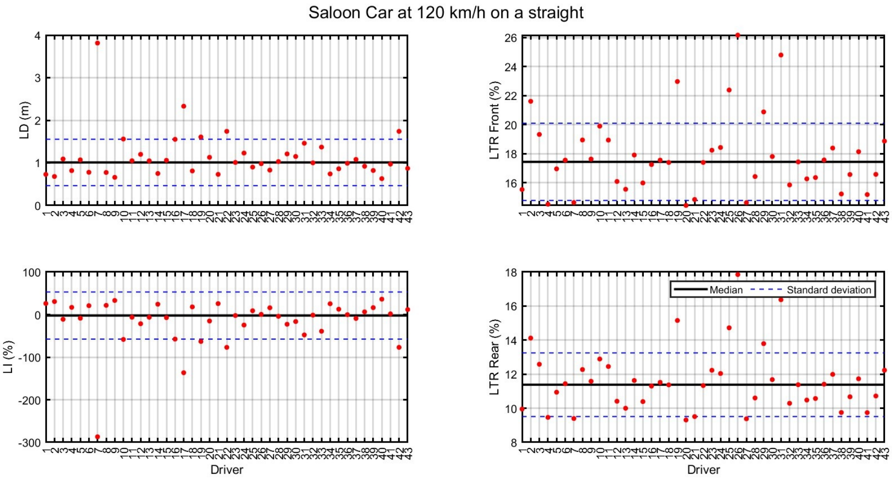

Figure 3.8: Performance distribution among drivers - Saloon Car at 120 km/h

Comparing the two vehicle types really similar lateral deviation outcomes are present, most values staying within 0.5 and 1.3 meters, but they result in different lane invasion values since as it was previously explained in Section 3 the width of the vehicle is used during the calculation of this indicator. It is probable that in the simulator environment the drivers are not fully aware of the width of the vehicle compared to a real-life scenario, this can also add to the intensity of the lane invasion in case of the lorry. It can also be observed that while in case of the saloon car the load transfer ratio generally produced higher values on the front axel on the contrary with the lorry configuration higher values emerged on the rear excel. This is probably due the position of the centre of gravity and the overall vehicle shape.

Figure 3.9 illustrates the risk index values extracted from the tests conducted with the empty lorry.

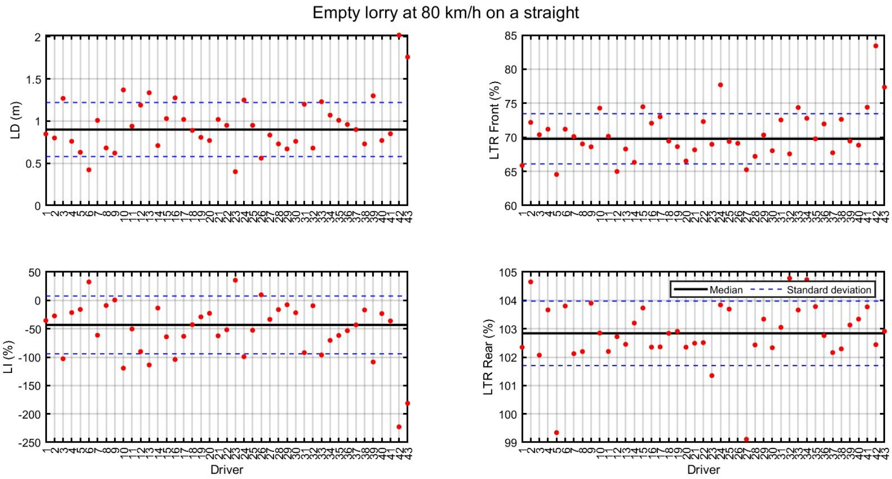

Figure 3.9: Performance distribution among drivers - Empty lorry at 80 km/h

The scenario employing the empty lorry was found the most dangerous scenario by 60% of the drivers. The combination of the extensive side surface area and relatively low weight resulted in quite poor handling behaviour for the empty lorry. As already discussed the lateral deviation does not show high sensitivity, but due to the reduced space between the border of the lane and the side of the vehicle the lane invasion is around -50% with almost all the drivers leaving the lane at least once. The load transfer ratio rached the highest values using this configuration, with staying between 65 and 75% on the front axle, and in almost all cases crossing the 100% threshold on the rear axle.

Figure 3.10 displays the risk index values conducted by employing the laden lorry.

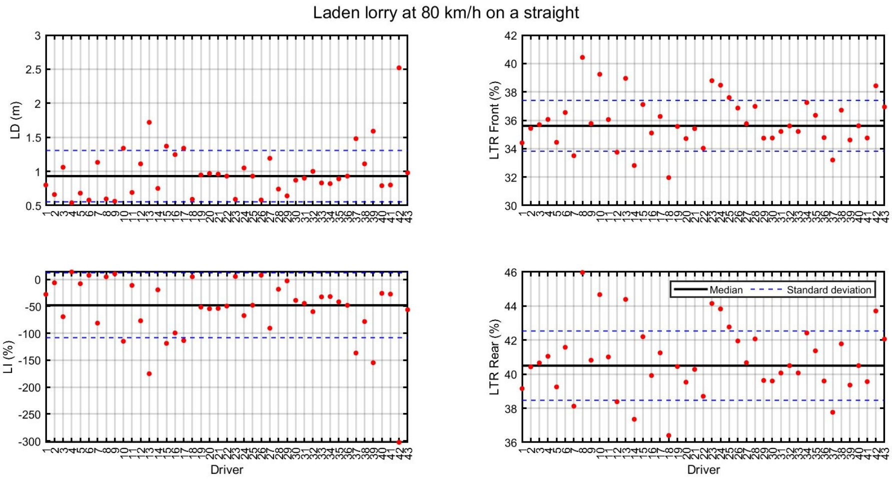

Figure 3.10: Performance distribution among drivers - Laden lorry at 80 km/h

Due to its heavier weight the laden lorry showed significantly better handling behaviours then the empty lorry, with good stability properties. This can be best observed by comparing the load transfer ratio values in Figure 3.9 and Figure 3.10. In case of the laden lorry the LTR values are 35-60% lower, staying far from the endangered zones. Lane invasion remains similar as in the empty case with the median being around 50%.

3.6. Chapter summary

This chapter presented the execution and outcomes of the Driver-in-the-Loop (DiL) experimental campaign conducted at the Politecnico di Milano driving simulator facility (DriSMi). By replacing the previously implemented PI controller with a human driver, the simulations enabled real-time interaction between driver and vehicle model, thereby capturing spontaneous behavioural responses under downburst wind excitation. The use of VI-CarRealTime ensured stable real-time performance without compromising immersion, which is essential for obtaining reliable behavioural data.

A total of 43 participants completed eight test conditions involving two vehicle categories: a Saloon Car in Part-Load configuration and a Small Lorry in both Empty and Laden states. Two trajectory types were considered: a straight 2 km layout and a curved configuration incorporating a 500 m radius semicircle, allowing both purely longitudinal and combined lateral-longitudinal dynamics to be assessed. All configurations were tested at a reference speed of 80 km/h, while additional higher-speed scenarios were included for the Saloon Car to reflect realistic operating conditions.

The experimental results demonstrated clear and physically consistent trends. Increased vehicle speed generally led to higher instability indicators, particularly in terms of load transfer ratio (LTR). Conversely, increased vehicle mass improved stability, as evidenced by the substantially lower LTR values recorded for the Laden Lorry compared with the Empty configuration. The Empty Lorry proved to be the most critical configuration, with frequent lane departures and rear axle LTR values exceeding the 100% threshold in several cases, highlighting its vulnerability to strong lateral wind excitation.

Interestingly, lateral deviation values remained relatively consistent across scenarios, suggesting that drivers actively compensated for disturbances to maintain lane position. However, this behavioural compensation often resulted in increased load transfer, underlining the importance of considering multiple risk indices simultaneously. Differences between front and rear axle load transfer trends further reflected the influence of vehicle geometry and centre-of-gravity position.

Although the test population was intentionally homogeneous in age and background to reduce variability, the dataset provides a robust and coherent foundation for subsequent PID controller tuning. The campaign successfully captured the distinct dynamic characteristics of each vehicle configuration and revealed the combined influence of speed, mass distribution, and aerodynamic exposure on vehicle stability under downburst conditions.

Overall, the driving simulator campaign delivered a structured and reproducible experimental framework, generating high-quality data that supports both controller calibration and a deeper understanding of vehicle–driver interaction in extreme wind scenarios.

04. Driver Controller Validation and Tuning

In this chapter, the validation and tuning of the PID controller is described. The controller was previously tuned based on less comprehensive test scenarios executed with the lorry type vehicle only exiting tunnels. As the first method, validation was performed on the basis of risk indices. Then for more accurate results the tuning was continued based on time-domain response analysis, with particular focus on lateral deviation, which is directly comparable with experimental driving data. The final tuning parameters were defined by this method primarily. Frequency domain analysis was additionally employed to interpret observed oscillations.

4.1. PID controller

The driver model implemented in this work is based on a PID control framework, which is widely adopted in vehicle dynamics simulations to reproduce path-following behaviour. However, the objective of the present study is not to achieve perfect trajectory tracking, but rather to reproduce a realistic driver response. For this reason, small residual tracking errors are considered acceptable and consistent with human driving behaviour.

Two tracking errors are defined for the path-following task: the distance error and the heading error with respect to the reference trajectory. The distance and heading errors are computed according to the geometrical configuration illustrated in 4.1. These errors are regulated by two separate controllers.

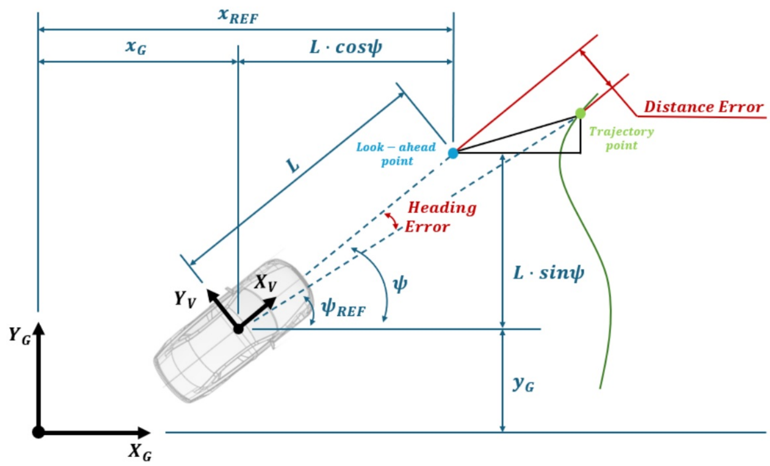

Figure 4.1: Heading and distance error representation

The distance error is controlled through a PI controller marked green on Figure 4.2, introducing both proportional and integral actions. The proportional term ensures prompt corrective steering action, while the integral term compensates for systematic deviations and steady-state offsets from the reference path. In contrast, the heading error is regulated by a purely proportional controller indicated with blue on the scheme, as integral action is not required to achieve satisfactory performance in this case. The derivative component is neglected for both errors. In practical implementations, derivative action is often avoided due to its sensitivity to noise and the additional filtering and tuning effort required, which increases system complexity without providing significant benefits for the objectives of this study.

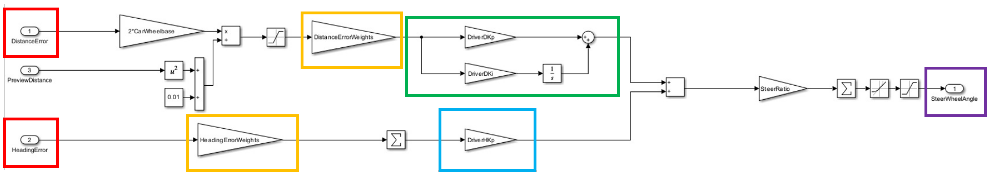

Figure 4.2: PID controller

A preview time is introduced to define a preview distance along the predefined trajectory. Based on this preview distance, a reference position is determined using look-up tables that describe the imposed path. In this way, distance and heading error are computed comparing the reference and actual position and heading of the vehicle. These will serve as the inputs for the PID controller, coloured red, while steering angle is the produced output framed in purple.

Different relative importance is assigned to the two error components, with the distance error considered more critical than the heading error. This is implemented through weighting gains in the control structure, with values of 0.75 and 0.25 for the distance and heading errors, respectively. These gains are highlighted in yellow on the picture of the PID controller.

The steering control is formulated under a kinematic steering assumption, meaning that the controller does not explicitly account for the full vehicle dynamics. This simplification is considered acceptable within the operating conditions investigated, as the dynamic vehicle model remains stable and follows the controller references with sufficient accuracy. More extreme situations, such as persistent actuator saturation, severe tyre grip loss, or aggressive braking manoeuvres, are outside the scope of the present simulations.

The behaviour of the driver model is therefore governed by four tuning parameters: the proportional gain associated with the distance error, the integral gain associated with the distance error, the proportional gain associated with the heading error, and the preview time. These parameters define the responsiveness and anticipatory characteristics of the simulated driver and are adjusted to obtain a realistic path-following performance.

The initial values of the controller gains were not determined within the present work, but were adopted from previous research conducted on the Small Lorry Empty configuration [40]. These values constitute the baseline setup used at the beginning of this study.

In the referenced work, the aerodynamic effects acting on the vehicle during tunnel exit manoeuvres were investigated. The simulated scenario consisted of a straight 2 km road including five tunnels, each with a length of 75 m. Upon exiting each tunnel, the vehicle was subjected to crosswind disturbances of varying peak intensity, namely 15 m/s, 20 m/s, and 25 m/s. The vehicle responses under these conditions were analysed and compared with driving simulator measurements.

The controller tuning in the referenced study was performed using the risk indices described in Section 2, namely the Lateral Deviation (LD) and the Load Transfer Ratio (LTR), as performance indicators. The resulting controller configuration did not satisfy all conditions with perfect accuracy, as it can be observed by comparing initial simulation values and experimental values in Tables 4.2, 4.4, 4.6 and 4.8. Nevertheless, it was considered an acceptable first approximation of driver behaviour.

In the present work, these previously calibrated parameters are used as the initial controller setup. A subsequent refinement of the gains is performed based on more accurate simulation results, as described in the following sections.

The initial parameters of the PID controller can be observed in Table 4.1

Proportional gain on distance error:	1.2
Proportional gain on heading error:	1.2
Integral gain on distance error:	4
Preview time:	1.5 s

Table 4.1: Initial tuning parameters

4.2. Validation

Based on the data collected during the driving simulator campaign it can be observed that the controller is performing significantly better than the human drivers in case of the sedan car. This is due to the fact that the controller was previously tuned based on simulations with a lorry type vehicle, which due to its weight, and side surface area requires stronger corrections from the driver than a smaller, lighter vehicle. This showed that the two different vehicles will require a different set of tuning parameters to mimic the drivers behaviour correctly.

The previously mentioned risk indices were calculated for each driver. In case of lateral deviation the highest value during the test was considered, which corresponds with the minimum value of the lane invasion. To investigate the moment with the highest possibility for a rollover also the maximum value of the load transfer ratio was evaluated.

For each test case, both the average and the median values of the risk indices were evaluated in order to account for inter-driver variability and to reduce the influence of extreme values. Although no faulty ones were identified among the straight scenarios during the experimental campaign, certain drivers exhibited more aggressive or more conservative behaviours, resulting in outlying risk index values. These cases were not excluded from the dataset, as they represent realistic, thought extreme driving styles. However, the arithmetic mean is sensitive to such values. For this reason, the median was considered with greater weight during controller validation, as it provides a more robust representation of the central tendency of the experimental population and better reflects typical real-world behaviour.

The objective of the parameter tuning was therefore to select controller gains such that the resulting risk index values lie within the experimental standard deviation range, while remaining slightly more conservative than the median driver response. This approach ensures that the controller behaviour remains representative of the experimental driver population without exceeding typical human performance. A controller acting significantly better than the majority of real-world drivers could introduce unrealistic system behaviour and potentially compromise the validity of the risk map developed in the final stage of the project.

During this method the controller parameters were continuously modified until closing the gap between the middle value of the risk indices obtained from the driving simulator campaign and the risk indices calculated based on the simulation. This method resulted in sufficient results but was not solely enough to optimize the parameters. Also the empty lorry showed very poor handling behaviour which encouraged the employment of other methods for tuning the controller. To tune the controller more precisely, the lateral displacement of the vehicles was plotted as a function of time.

All the examined scenarios follow a simple straight trajectory with a length of 2 km. The wind simulation started 30 seconds after the initiation of the test, but this part was removed since it is irrelevant for the validation of the controller as we were curious about how well it is able to compensate for the effects of the wind. On Figures 4.3, 4.4, 4.5 and 4.6 the thin colourful lines each represent one of the 43 test drivers. The thicker red line shows the performance of the PID controller. The straight black lines are the borders of the lane, considering the average Italian lane width of 3.75 m. Significant oscillations can be observed around 0 which is the centre of the lane. The general target was to try to keep the oscillations in the simulation on a level which visually appears similar to the trajectory of average drivers.

4.2.1. Saloon Car

In case of the saloon car there were two test cases, one with 80 km/h and the second with 120 km/h. While initially the goal was to find a common set of parameters for both test cases, it became clear that one set is insufficient to satisfy the requirements for both scenarios. Using the same gains with different preview times proved inadequate, as the smooth adaptation exhibited by real drivers cannot be replicated by modifying a single parameter. Therefore, it was necessary to use a completely different set of parameters for the two test cases.

For the 80 km/h scenario, the risk indices calculated from the experimental data can be seen in the first row of Table 4.2. It can be observed that the gap between the initial simulation data and the experimental data is quite significant. This is due to that the first tuning happened on a lorry type vehicle as it was previously mentioned. In the fourth row of Table 4.2, the risk indices calculated after the tuning are displayed, they fall much closer to the experimental values.

	LD	LI	LTR front	LTR rear
Experimental median	0.870	11.7%	13.0	8.3
Experimental standard deviation	0.379	38.5%	2.4	1.6
Simulation initial	0.190	80.7%	10.8	6.8
Simulation tuned	0.874	11.3%	14.5	9.2
Error	-0.004	0.4%	-1.5	-0.9

Table 4.2: Risk indices Saloon car at 80 km/h

In Figure 4.3, the lateral deviation-time function is shown. The thicker red line, representing the simulation, blends in among the real drivers, showing similar patterns.

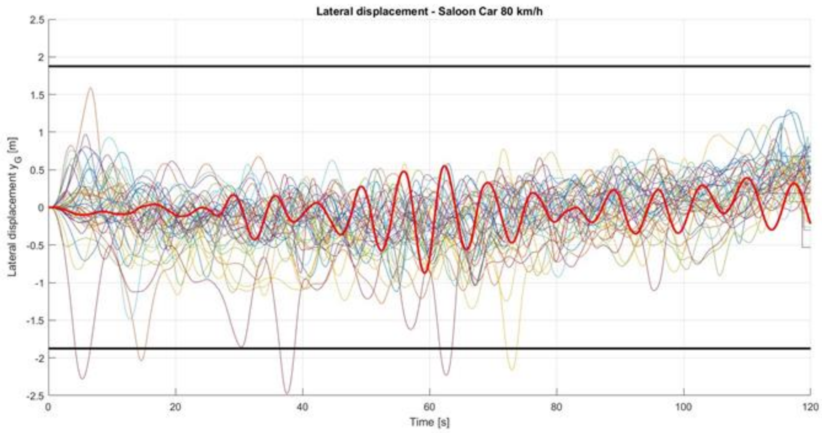

Figure 4.3: Lateral deviation as a function of time - Saloon car at 80 km/h

Based on this analysis, the set of parameters shown in Table 4.3 is considered validated.

	Initial	Tuned
Proportional gain on distance error:	1.2	0.4
Proportional gain on heading error:	1.2	0.4
Integral gain on distance error:	4	0.8
Preview time:	1.5 s	1.4 s

Table 4.3: Tuning parameters Saloon car at 80 km/h

The same method was conducted in case of the 120 km/h scenario. As expected the final tuning parameters resulted in higher gains and shorter preview time compared to the 80 km/h scenario, displayed in Table 4.4. It can be observed the 1.4 seconds preview time in case of the 80 km/h scenario and the 0.9 seconds preview time at 120 km/h both correspond to an approximately 30 meters of preview distance. In case of the front load transfer ratio the error slightly exceeds the standard deviation but it is considered acceptable because as it could be seen in the previous chapter even some of the drivers fall outside of the range set up by the standard deviation.

	LD	LI	LTR front	LTR rear
Experimental median	1.008	-2.3%	17.4	11.4
Experimental standard deviation	0,539	54.7%	2.6	1.8
Simulation initial	0.428	56.5%	14.3	9.2
Simulation tuned	1.014	-2.9%	20.2	13.1
Error	-0.006	0.6%	-2.8	-1.8

Table 4.4: Risk indices Saloon car at 120 km/h

Figure 4.4 illustrates the lateral deviation values as a function of time belonging to 120 km/h scenario of the Saloon car.

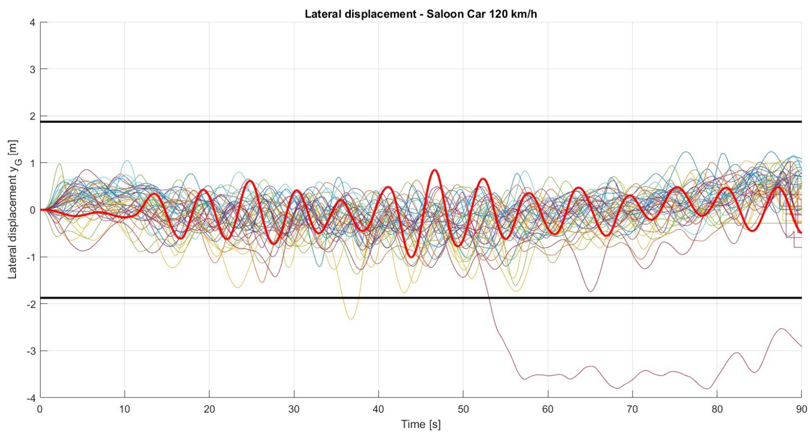

Figure 4.4: Lateral deviation as a function of time - Saloon car at 120 km/h

Table 4.4 contains the final tuning parameters for the Saloon Car travelling at the speed of 120 km/h.

	Initial	Tuned
Proportional gain on distance error:	1.2	0.5
Proportional gain on heading error:	1.2	0.5
Integral gain on distance error:	4	0.9
Preview time:	1.5 s	0.9 s

Table 4.5: Tuning parameters Saloon car at 120 km/h

4.2.2. Empty lorry

While adjusting the parameters, it also showed that the lorry in empty and laden conditions has to be handled separately, this observation aligned well with the experience of the real drivers who participated in the driving simulator campaign.

The empty lorry emerged to be the biggest challenge for both real drivers and for proper tuning of the controller. The relatively large side surface area and the low weight resulted in poor handling properties.

This vehicle configuration required the highest tuning parameters, higher gains on both the distance error and heading error. On the contrary the preview time is slightly lower then in the other two scenarios at 80 km/h since more direct corrections were necessary for the handling of this vehicle. The error between the risk indices calculated based on the simulation and the experimental data are below the standard deviation in every case except the rear load transfer ratio, where the simulation resulted in a marginally higher value than the experimental median, but for safety reasons this outcome was aimed at and considered acceptable. The described indices can be observed in Table 4.6.

	LD	LI	LTR front	LTR rear
Experimental median	0.895	-43.2%	69.8	102.8
Experimental standard deviation	0.317	50.7%	3.6	1.1
Simulation initial	1.163	-86.1%	66.1	105.6
Simulation tuned	0.932	-49.1%	66.7	105.5
Error	-0.037	5.9%	3.0	-2.6

Table 4.6: Risk indices Small Lorry in Empty condition at 80 km/h

On Figure 4.5 lateral displacement of the vehicle is presented. When inspecting the overall shape of the plot a slight delay can be observed in the experimental data compared to the red line of the simulation. This delay is due to that the empty lorry lacked friction during the simulator campaign therefore not being able to maintain the 80 km/h target at the later part of the scenario. It is still clearly displayed that the overall shape produced by the simulation is almost identical to the experimental data, therefore it is satisfactory approximation of a real driver.

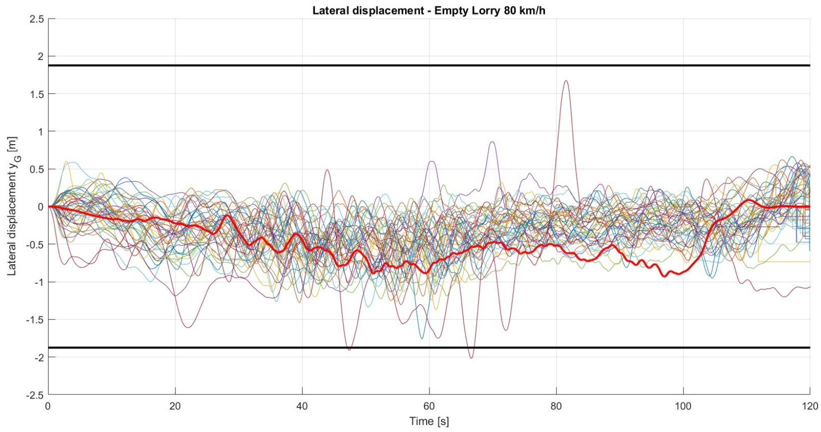

Figure 4.5: Lateral deviation as a function of time - Small Lorry in Empty condition

The final tuning parameters of the Empty Lorry are presented in Table 4.7. This configuration was the closest to the initial tuning parameters of the controller.

	Initial	Tuned
Proportional gain on distance error:	1.2	1.2
Proportional gain on heading error:	1.2	1.2
Integral gain on distance error:	4	2
Preview time:	1.5 s	1.2 s

Table 4.7: Tuning parameters Empty lorry at 80 km/h

4.2.3. Laden lorry

Due to its heavier weight the laden lorry showed significantly better handling behaviours then the empty lorry, with good stability properties. In Table 4.8 the risk index values used for the tuning of the laden lorry controller are listed.

	LD	LI	LTR front	LTR rear
Experimental median	0.925	-48.0%	35.6	40.5
Experimental standard deviation	0.372	59.6%	1.8	2.0
Simulation initial	0.685	-9.6%	33.1	37.7
Simulation tuned	0.979	-56.7%	37.1	42.2
Error	-0.054	8.7%	-1.5	-1.7

Table 4.8: Risk indices Small Lorry in laden condition at 80 km/h

In case of all the risk indices the error stays below the standard deviation by the controller slightly underperforming the the real drivers. The same 1.4 s preview time gave the closest result to the experimental data that was used for the saloon car at 80 km/h, emphasizing the main correlation between vehicle velocity and this tuning parameter. The other gains are much lower than in case of the empty lorry, rather being closer to the saloon car. On Figure 4.6 the lateral position of the vehicle is plotted. The red simulation line fits the experimental data completely evaluating both the overall shape and the oscillations.

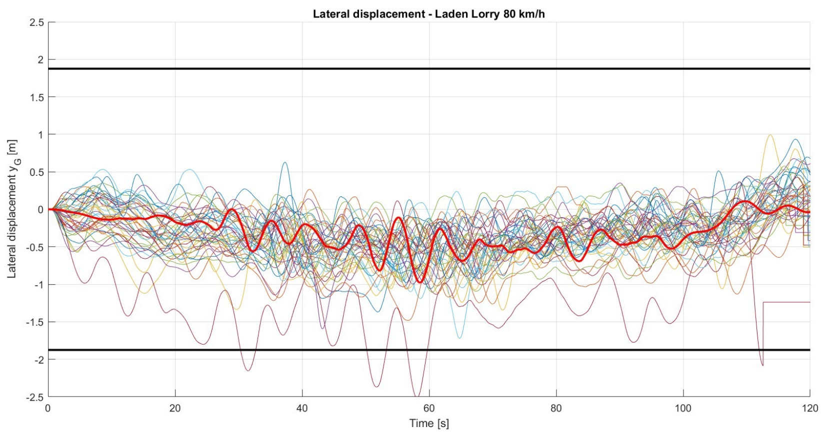

Figure 4.6: Lateral deviation as a function of time - Small Lorry in Laden condition

The final tuning parameters for the Laden Lorry configuration are displayed in Table 4.9.

	Initial	Tuned
Proportional gain on distance error:	1.2	0.5
Proportional gain on heading error:	1.2	0.5
Integral gain on distance error:	4	1
Preview time:	1.5 s	1.4 s

Table 4.9: Tuning parameters Laden lorry car at 80 km/h

Figure 4.7 shows a comparison between the three vehicle configurations analysed at 80 km/h. From left to right the risk indices of the saloon car, the empty lorry and the laden lorry are displayed starting from the top with lateral deviation then front and rear load transfer ratios. The figure uses a complex scheme, all the experimental results are indicated with crosses, often overlapping each other, the highest and lowest value is highlighted with a black horizontal line. The median of the experimental values is represented by the longer red line, while the results obtained from the simulation are marked by the blue dot. This plot also visually confirms how well the simulations imitate the experimental data.

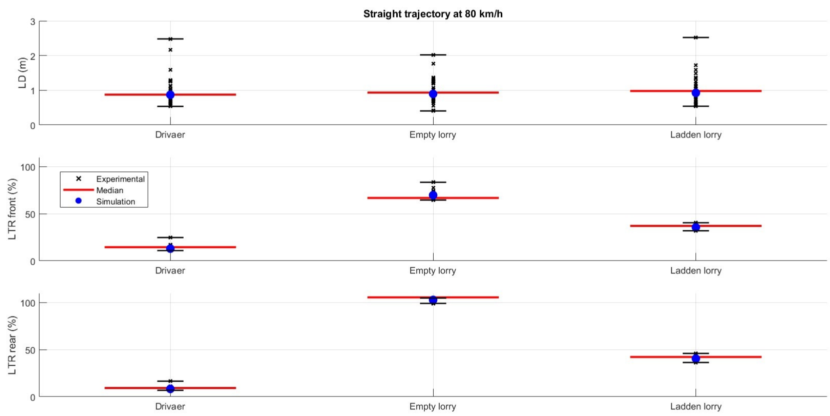

Figure 4.7: Summary of risk indices at 80 km/h

4.3. Frequency domain analysis

To gain a deeper understanding, an analysis in the frequency domain was also conducted. This helped to recognise the source of the oscillations, and to justify the results achieved with the previously described methods. The investigation which employed FFT and PSD methods revealed two peaks in the frequency domain. The first one was steadily around 0.01 Hz corresponding to a signal with a wavelength of 100 seconds which covers the whole duration of the simulation. So this peak is the overall trend in the simulation, it shows how much the vehicles are laterally displaced by the wind. On the other hand, the second peak's locations varied from vehicle to vehicle, even from driver to driver. It is caused by the combined effect of the wind's frequency, the driver's reaction time, or preview time in case of the controller and handling behaviour of the vehicle. The placement of this second peak contributed to the adjustment of the preview time of the controller, but the other two methods defined the final parameters primarily.

4.4. Chapter summary

This chapter presented the validation and systematic retuning of the PID-based driver controller for the different vehicle configurations considered in this study. The initial controller parameters, inherited from previous work conducted exclusively on the small lorry in empty configuration during tunnel exit manoeuvres, were adopted as a baseline. While these parameters provided an acceptable first approximation, the broader set of scenarios and vehicles investigated in the present work revealed clear limitations in their general applicability.

Validation was first performed using risk indices, namely Lateral Deviation (LD), Lane Invasion (LI) and Load Transfer Ratio (LTR) at the front and rear axles. The simulation results and the experimental driving simulator campaign outsomes were compared, considering both the arithmetic mean and, more importantly, the median values of the experimental population. The median turned out as a more robust indicator of typical driver behaviour, as it reduces the influence of extreme but realistic driving styles. The objective of the tuning process was therefore to ensure that simulated results lie within the experimental standard deviation while remaining slightly more conservative than the median driver response, thereby avoiding unrealistically optimal behaviour.

Although risk index comparison provided a solid foundation for validation, an additional method was applied. The time-domain analysis of the lateral displacement was introduced to achieve a more refined calibration. By visually comparing the simulated trajectories with those of the 43 experimental drivers.

The results demonstrated that a single set of controller parameters is not adequate across different vehicle types and operating conditions. For the saloon car, distinct parameter sets were required for 80 km/h and 120 km/h, highlighting the strong relationship between vehicle speed and preview time. In both cases, substantial improvements were achieved compared to the initial configuration, with the tuned controller blending into the envelope of experimental driver trajectories. The highest relative improvement was observed for the saloon car, where the initial controller clearly overperformed compared to real drivers.

The empty lorry represented the most challenging case due to its unfavourable mass-to-side-area ratio and consequently poor crosswind stability. Higher control gains and a shorter preview time were necessary to reproduce realistic behaviour. Despite minor deviations in certain LTR values, the final configuration achieved a satisfactory balance between accuracy and conservativeness.

In contrast, the laden lorry exhibited better stability properties, requiring lower gains and a preview time similar to that of the saloon car at 80 km/h. The tuned results showed strong agreement with experimental data across all evaluated indices, both numerically and in terms of trajectory shape.

Finally, frequency-domain analysis provided additional insight into the origin of the observed oscillations. Two dominant frequency components were identified: a low-frequency component representing the overall wind-induced displacement trend, and a higher-frequency component influenced by wind characteristics, vehicle dynamics and driver reaction (preview) time. Although this analysis supported the selection of preview time, it primarily served as an interpretative tool.

Overall, the retuning process significantly improved the realism and representativeness of the driver model across all vehicle configurations. The resulting parameter sets ensure that the simulated driver behaviour closely reflects experimental observations, thereby providing a reliable base for the execution of the subsequent developments.

05. Risk Assessment through sensitivity analysis

With the refined PID controller a sensitivity analysis was carried out to setup a risk map of different wind magnitudes and directions. In this chapter the tested configurations are described, and the results obtained from the analysis are discussed. The goal is to verify the capabilities of the model to effectively represent diverse conditions and to analyse the effect of them in vehicle stability. In particular the relative direction between the storm and the vehicle trajectory, and the intensity of the storm were covered in this analysis.

5.1. Analysed scenarios

For this analysis only straight scenarios were tested the direction ranged from only 0 to 180, because the other side would be symmetric. It increases in 10 degrees increments, making it a total of 19 different wind angles. The wind speed increases from 15 m/s to 35 m/s with 5 m/s steps. The applied wind profiles, as previously, generated by the research team at University of Genoa, are displayed in Figure 5.1.

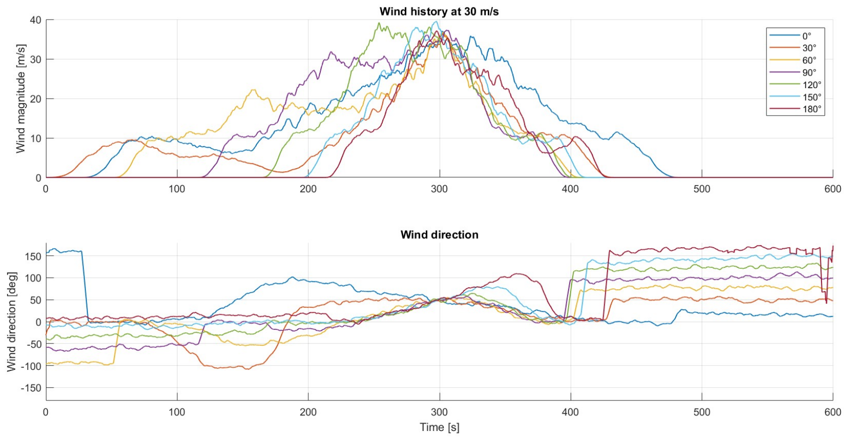

Figure 5.1: Wind histories at 30 m/s

As an example the 30 m/s wind was chosen, but for the sake of clarity only every third wind direction is represented on this plot. We can see the significant difference in the shape of both the wind magnitude and direction curves. On Figure 5.2 the reverse approach was applied, all the wind speeds from 15 m/s to 35 m/s are plotted which are attacking from a 90 degree angle. We can see here that the overall shape of the curves is really similar, they only differ in magnitude.

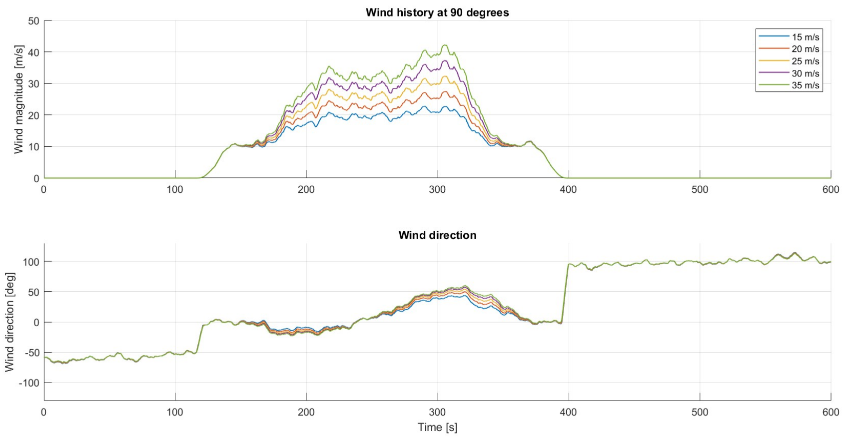

Figure 5.2: Wind histories at 90 degrees

To interpret the intensity of the wind better, the applied magnitudes are showcased in Table 5.1 with the corresponding categories on the Beaufort scale [41].

15 m/s	Near gale
20 m/s	Gale
25 m/s	Storm
30 m/s	Violent storm
35 m/s	Hurricane

Table 5.1: Wind intensities on Beaufort scale

The tests were conducted with two different type of vehicles, the saloon car and small lorry. In case of the small lorry two different weight configurations were tested, since previous tests showed that it is a highly relevant influencing factor.

For this analysis the velocity of the vehicles were defined at a constant speed of 100 km/h. As presented in the previous chapter the PID controller was tuned at different speeds. As for the saloon car the PID controller has tuning parameters both at 80 km/h and 120 km/h, the interpolation of these parameters resulted in the corresponding values to 100 km/h. Regarding the small lorry, the controller was only tuned at 80 km/h so the tuning parameters were modified assuming direct proportionality with the saloon car. Therefore the following tuning parameters were used to carry out this sensitivity analysis.

	Saloon car	Empty lorry	Laden lorry
Proportional gain on distance error:	0.45	1.35	0.5625
Proportional gain on heading error:	0.45	1.35	0.5625
Integral gain on distance error:	0.85	2.125	1.0625
Preview time:	1.15 s	0.986 s	1.15 s

Table 5.2: Tuning parameters used at 100 km/h

5.2. Results

The safety thresholds remained the same as used in previous chapters, 1 m for the saloon car and 0.625 m for the lorry regarding lateral deviation, and 100% for the load transfer ratio for both vehicle types. It was already pointed out in Chapter 3.5 that a load transfer ratio of 100% does not necessary cause a rollover. In case of the saloon car the load transfer ratio obtained from the front axle is displayed and for the lorry the rear axle produces more significant values therefore that is displayed on the plots. Even though significant differences are present between the vehicles it was chosen to use the same scaling for all the plots to make them directly comparable. Since this made some of the values hard to read the full tables containing the risk indices are added in the appendix.

In some cases, the simulations produced extremely large values of lateral deviation and load transfer ratio. Consequently, the risk indices were saturated at predefined limits to allow consistent visualisation across all scenarios. For LD, this saturation value was set to 2 m, while for LTR it was set to 120%. Even though all scenarios exceeding the preset safety threshold are considered dangerous, in case of the saturated values these conditions would most certainly result in road accidents, as either causing the vehicle to rollover or completely abandoning the lane.

The trend of all vehicles exhibiting higher LD and LTR values at higher angular values, is due to the peak wind values achieved at each angle, which are shown on Figure 5.3 as an example at 30 m/s absolute wind speed.

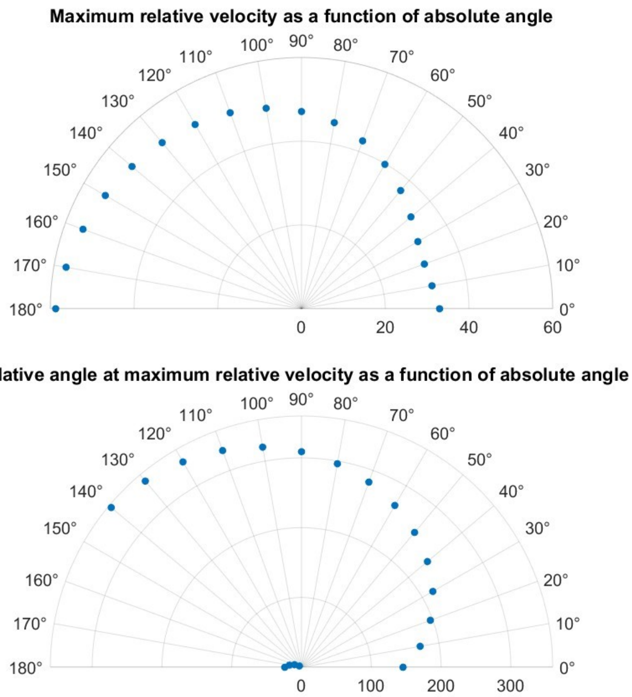

Figure 5.3: Peak Relative Wind Speed and Angle as a function of vehicle heading

5.2.1. Saloon Car

In Figure 5.4 the results corresponding to the LD index for the saloon car are presented. In the figure the values obtained are shown in a polar plot where angles corresponds to the trajectory-storm angle while the different curves correspond to the different wind intensities analysed.

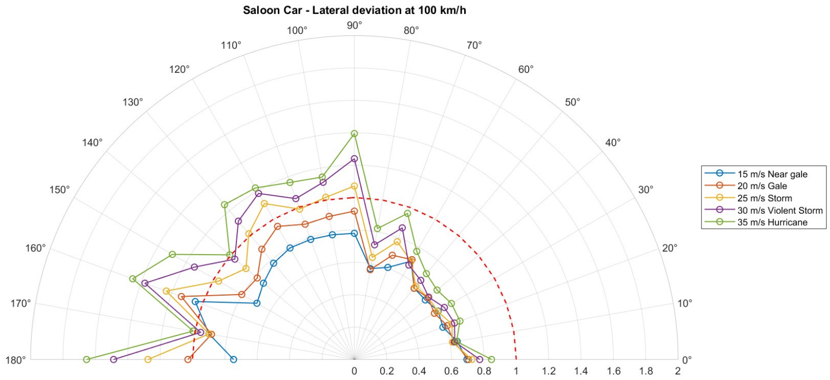

Figure 5.4: Lateral deviation of Saloon Car

For the saloon car, the lateral deviation (LD) does not always increase proportionally with wind magnitude. A trend can be observed at lower angles (mostly under 60°) in Figure 5.4, where the LD appears relatively insensitive to storm intensity. It is important to remember that value of wind speed presented in the plots is related to the storm intensity. The fact that an increasing storm intensity is not being traduced into a bigger risk can be explained considering that for the aerodynamic loads what matters is the relative wind velocity. In this case, because of the direction of wind in the absolute reference frame, the increment of wind speed is not directly traduced in a larger relative wind. The indicated velocity on the plots correspond to the absolute wind velocity, as we can observe on Figure 5.5 in some cases, especially at lower angles a lower absolute wind speed can produce higher relative velocity. The LD values of 15 and 20 m/s stay mostly below the threshold, in cases of higher velocities only angles above 90° cross the 1 m threshold, reaching the peak value of 1.65 m at 180°.

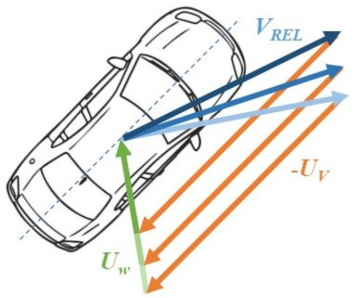

Figure 5.5: Relative velocity presentation

In Figure 5.6 the load transfer ratio values are shown for the Saloon car using the same scheme as for LD.

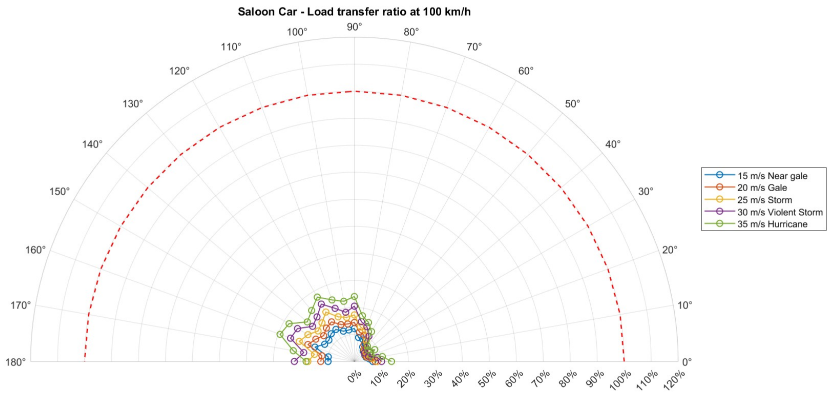

Figure 5.6: Load transfer ratio of Saloon Car front axle

All the load transfer ratio values stay well bellow the safety thresholds, reaching no more than 30%. This means that the saloon car shows a low probability for rollover even under extreme wind conditions. On the contrary to LD the load transfer index seems to response to wind velocity more linearly.

5.2.2. Empty Lorry

In Figure 5.7 the lateral deviation values belonging to the empty lorry configuration are introduced.

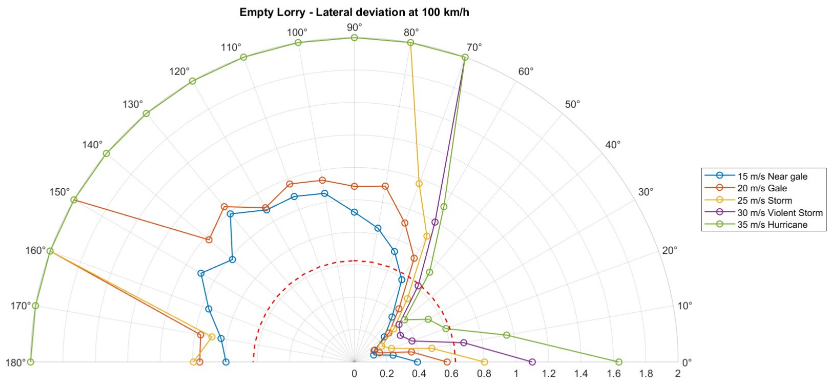

Figure 5.7: Lateral deviation of Empty Lorry

Values of lateral deviation only stayed below the set threshold at lower angles, until 50 and 70 degrees depending on the wind intensity. Only the 15 m/s curve has no saturated values, but even that travels far from the 0.625 m semicircle corresponding to the border of the lane.

The load transfer ratio belonging to the rear axle of the Empty Lorry is displayed on Figure 5.8.

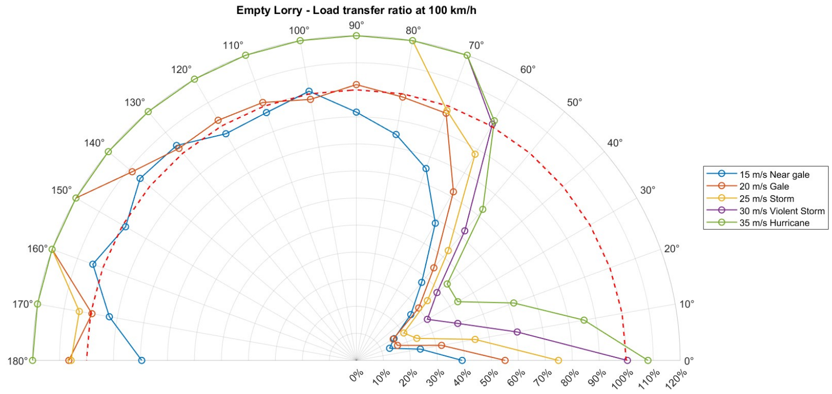

Figure 5.8: Load transfer ratio of Empty Lorry rear axle

In case of the empty lorry the biggest threat is seen as the rollover, mostly presented by the load transfer ratio. At speeds of 25, 30 and 35 m/s configurations with angles starting from 70-80° all lead to the vehicle to rollover. While at 20 m/s most of the risk index values rest on or around the safety threshold, although at particular angles it also resulted in rollover. While with 15 m/s wind intensity the load transfer values stayed mostly in the safe zone.

The empty lorry configuration generally develops the highest risk index values among the tested vehicle configurations. The driving of this vehicle type cannot be considered safe even during the influence 15 m/s wind considering both lateral deviation and load transfer as it can be observed on Figures 5.7 and 5.8. All the wind intensities above resulted in extremely dangerous scenarios.

5.2.3. Laden Lorry

Figure 5.9 and 5.10 illustrates the lateral deviation and load transfer ratio results for the laden lorry configuration, respectively.

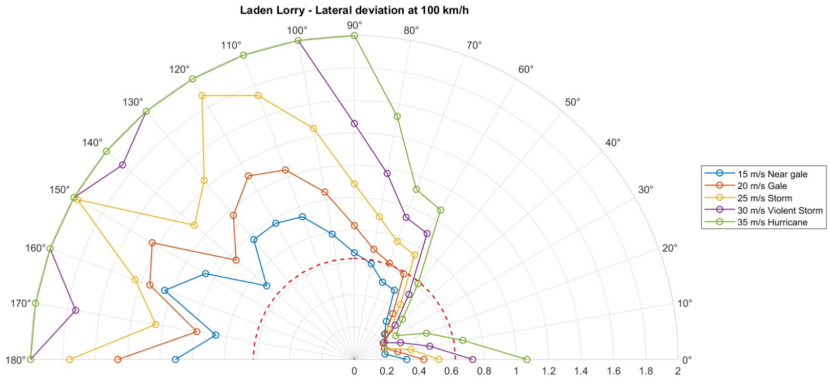

Figure 5.9: Lateral deviation of Laden Lorry

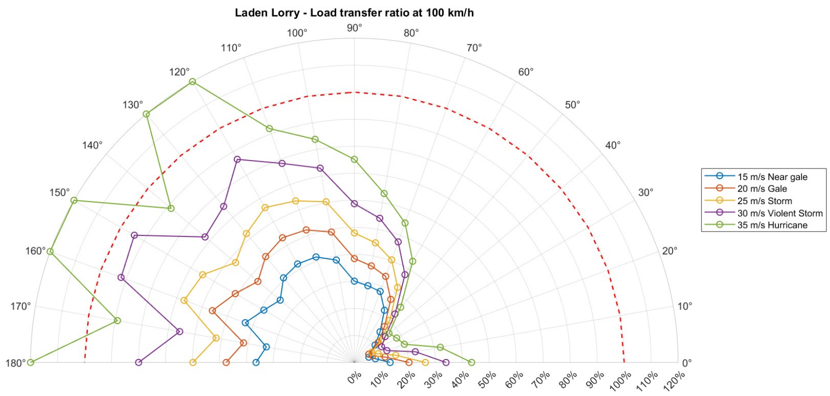

Figure 5.10: Load transfer ratio of Laden Lorry rear axle

While except at 35 m/s LTR values stayed below the safety threshold, not exposing significant risk, lateral deviation values overcame the 0.625 meter threshold as low as 15 m/s, and approaching the absolutely critical value of 2 m at 25 m/s. The LD values stayed below the threshold only between angles of 0 and 80 degrees, this span seems to be less sensitive to wind intensity.

Some particular cases at the relative speed of 35 m/s lead to rollover, namely 120, 130, 150, 160 and 180 degrees. Many of the surrounding vales both regarding velocity and angles, resulted in LD values above 2 meters which can mean either abandoning the road or providing possibility to frontal crashes, being just as dangerous as the rollover scenarios, therefore also labelled as outmost critical.

Regardless the laden lorry proved to be significantly more stable than the empty configuration, further confirming the necessity of testing the two loading conditions separately. With this vehicle configuration the primary risk proved to be the lane deviation not rollover in contrary with the empty lorry.

Both lorry configurations exhibit a monotonically increasing trend in LD and LTR with wind magnitude. This behaviour contrasts with the saloon car case, where such monotonicity is observed only for LTR, while LD shows a weaker dependence on wind magnitude. A possible explanation for this difference lies in the aerodynamic characteristics of the two vehicle types. In the case of the lorry, the aerodynamic coefficients vary continuously with the relative wind angle, resulting in a consistent increase in aerodynamic loads as wind magnitude rises. Conversely, for the saloon car, the aerodynamic coefficients present a discontinuity. This suggests that the relative wind angle, rather than wind magnitude alone, plays a key role in determining the vehicle response.

5.3. Chapter summary

This chapter presented the results of a sensitivity analysis aimed at evaluating the safety performance of different vehicle configurations under varying wind magnitudes and directions. The analysis was conducted using a refined PID controller and focused on constructing a risk map based on lateral deviation and load transfer ratio indicators.

Three vehicle configurations were investigated: a saloon car, an empty lorry, and a laden lorry, all tested at a constant vehicle speed of 100 km/h. The angle between the car trajectory and the storm motion ranged from 0° to 180° with 10° increments, while wind magnitudes varied between 15 m/s and 35 m/s in 5 m/s steps.

The results showed distinct behavioural differences among the vehicle configurations. The saloon car exhibited relatively low sensitivity to wind magnitude in terms of lateral deviation, while load transfer ratio responded more proportionally to increasing wind intensity. The lorry configurations demonstrated higher overall risk indices, with the empty lorry showing the most critical behaviour, including rollovers. In contrast, the laden lorry proved to be significantly more stable, though higher risk values were still observed at larger wind angles.

Risk indices generally tended to increase toward higher wind direction values, indicating the elevated danger when moving opposite to storm movement.

Overall, the sensitivity analysis confirmed the strong influence of both wind magnitude and direction on vehicle stability and highlighted the importance of considering loading conditions when assessing wind-induced risk.

Given the infinite range of possible configurations, it is difficult to draw fully general conclusions. However, the developed tool is capable of accurately reproducing any given scenario. Therefore, the method can be extended to investigate specific events or conditions such as bridges, embankments, or viaducts, in order to assess how critical these situations may become and to evaluate potential mitigation measures.

06. Conclusions and future developments

6.1. Conclusions

In this thesis, a simulation-based framework for analysing the stability of road vehicles under crosswind conditions was further developed and refined. In particular, the driver model was calibrated and validated using data collected during an experimental campaign conducted at the DriSMi facility of Politecnico di Milano. The validated model was then employed to investigate different vehicle configurations and wind intensities, assessing its capability to reproduce diverse operating conditions and their effects on vehicle stability. An extensive sensitivity analysis was conducted employing different vehicle configurations and wind intensities, forming the basis for the development of a risk map.
Based on this, the following conclusions can be drawn.

6.1.1. Driving Simulator Campaign

During the simulation campaign the Saloon Car proved better handling behaviour and higher stability properties, than the Small Lorry. The lorries exhibited higher load transfer values on the rear axle, on the contrary the sedan car on the front axle. Critical values in load transfer were only reached with the Empty Lorry configuration. Lateral deviation stayed constant across all vehicle types, but due to different vehicle width caused higher risks for the lorry type vehicle.

The straight-road scenarios provided a consistent framework for comparison and later tuning of the controller.

6.1.2. Driver Controller Validation and Tuning

It was found that one set of tuning parameters cannot cover different vehicle configurations and modalities, therefore the employment of an adaptive controller was required. As the scenarios in experimental campaign mainly focused on varying vehicle types, vehicle weights and vehicle speeds it was possible to adapt the controller to these parameters.

The adaptation happened through the evaluation of risk indices. It was avoided to tune the controller in a way that it outperforms the real drivers, to ensure its credibility for the risk map generation. Additionally to the risk index evaluation a visual method was also adapted for behavioural validation. During the tuning process high correlation was found between the vehicle speed and the preview distance, an approximate 30 meters preview distance was observed across different speeds.

6.1.3. Risk assessment

The sensitivity analysis confirmed that crosswind-induced risk strongly depends on vehicle configuration, wind magnitude, and wind direction. Using predefined thresholds for lateral deviation and load transfer ratio, critical scenarios were identified based on safety thresholds defined as 100% of load transfer ratio or lateral deviations exceeding 1 m in case of the saloon car and 0.625 m for the small lorry.

The saloon car showed the lowest overall sensitivity to crosswinds. Load transfer ratios remained well below the limits in all cases, indicating negligible rollover risk. Lateral deviation exceeded the 1 m threshold mainly at higher wind angles and magnitudes. The dependence of lateral deviation on wind magnitude was not strictly monotonic which was explained by the composition of relative velocity.

The empty lorry configuration exhibited the most critical behaviour confirming that the empty loading condition is highly vulnerable to crosswind disturbances. Except at the lowest wind magnitude, most scenarios exceeded safety thresholds, with rollover representing the dominant risk mechanism.

The laden lorry demonstrated significantly improved rollover stability compared to the empty configuration. However, lateral deviation emerged as the primary risk factor, exceeding critical values at higher wind magnitudes and larger angles. This indicates that increased mass reduces rollover susceptibility but does not eliminate the risk of severe lateral instability.

Overall, the results demonstrate that wind direction is as decisive as wind magnitude, and that loading condition fundamentally alters vehicle response. The results provide a structured representation of these interactions and clearly identify the empty lorry as the most critical configuration under the investigated conditions.

6.2. Future developments

Future work could focus on extending the controller adaptability across a wider range of operating conditions. In particular, additional experimental campaigns could be conducted at different vehicle speeds, especially for the lorry configuration, in order to enable interpolation of the tuning parameters across the velocity domain. While the present study demonstrated satisfactory performance at 80 km/h and 120 km/h for the saloon car, expanding simulator testing to include at least two lorry-specific speed conditions would further improve the robustness of the parametrisation and reduce the dependence on discrete tuning points.

Furthermore, the controller could be enhanced to account for variations in wind intensity. Although wind magnitude was not explicitly varied during the experimental campaign, the results suggest that human drivers tend to regulate steering actions to maintain relatively stable lateral displacement across different vehicle configurations. This behaviour indicates that driver adaptation mechanisms may mitigate the influence of increasing wind intensity, particularly on lateral deviation, whereas load transfer ratio may exhibit stronger sensitivity to aerodynamic loading. However, additional experimental campaigns involving different wind intensities would be necessary to reliably characterise these effects and to support the development of adaptive control strategies. Consequently, future developments could investigate adaptive control strategies capable of adjusting controller parameters in response to changing wind conditions, thereby reproducing more closely the compensatory behaviour observed in real drivers.

In addition, the proposed methodology could be extended to investigate the response of autonomous driving systems under crosswind disturbances. The current framework, which integrates a high-fidelity vehicle model with a driver behavioural controller validated through simulator experiments, provides a suitable basis for replacing the human driver model with autonomous control algorithms. For instance, lateral control strategies based on preview control, model predictive control (MPC), or LQR techniques could be implemented and compared under identical downburst wind scenarios. This would enable a systematic assessment of how automated steering systems react to highly transient and localised wind fields, such as those reconstructed within the CROSS-STORM framework.

Finally, the experimental campaign could be expanded to include a more diverse driver population, with particular attention given to age distribution and driving experience. Special emphasis could be placed on drivers with heavy vehicle driving experience, as the lorry involved scenarios were identified as the most critical in terms of risk exposure. Since heavy vehicle driving is typically associated with professional driving activity in real-world conditions, evaluating the response of drivers with specific lorry handling experience would be particularly valuable. In the present campaign, most participants were relatively young drivers with limited or no experience in lorry driving, which may have influenced the observed results. Investigating how professional driving experience affects cross-wind handling behaviour could therefore provide additional insight into population variability.

Bibliography

[1] A. Cioffi, A. Raghu Prakash, E. Sabbioni, M. Vignati, and F. Cheli, "Heavy-vehicle response to crosswind: Evaluation of driver reactions using a dynamic driving simulator," *Vehicles*, vol. 5, no. 1, pp. 344–366, 2023.

[2] D. Sekulić, A. Vdovin, B. Jacobson, S. Sebben, and S. M. Johannesen, "Analysis of vehicle path tracking ability and lateral stability on a floating bridge under a crosswind," *Journal of Wind Engineering and Industrial Aerodynamics*, vol. 105070, p. 105070, 2022.

[3] N. Winkler, L. Drugge, A. Trigell, and G. Efraimsson, "Coupling aerodynamics to vehicle dynamics in transient crosswinds including a driver model," *Computers Fluids*, vol. 138, 08 2016.

[4] N. Becker, H. W. Rust, and U. Ulbrich, "Weather impacts on various types of road crashes: a quantitative analysis using generalized additive models," *European Transport Research Review*, vol. 14, no. 1, p. 37, 2022.

[5] X. Zhang and C. Proppe, "Risk assessment of road vehicles under wind gust excitation," *Journal of Computational and Nonlinear Dynamics*, vol. 15, 06 2020.

[6] J. Huemer, T. Stickel, E. Sagan, M. Schwarz, and W. A. Wall, "Influence of unsteady aerodynamics on driving dynamics of passenger cars," *Vehicle System Dynamics*, vol. 52, no. 11, pp. 1470–1488, 2014.

[7] H. R. Byers and R. R. Braham, "Thunderstorm structure and circulation," *Journal of Atmospheric Sciences*, vol. 5, no. 3, pp. 71 – 86, 1948.

[8] M. Yu, Y. Xu, W. Fang, *et al.*, "Crosswind stability evaluation of high-speed train using different wind models," *Chinese Journal of Mechanical Engineering*, vol. 32, no. 1, 2019.

[9] C. Junayed, C. Jubayer, D. Parvu, D. Romanic, and H. Hangan, "Flow field dynamics of large-scale experimentally produced downburst flows," *Journal of Wind Engineering and Industrial Aerodynamics*, vol. 188, pp. 61–79, 2019.

[10] L. Carassale and G. Solari, "Monte carlo simulation of wind velocity fields on complex structures," *Journal of Wind Engineering and Industrial Aerodynamics*, vol. 94, no. 5, pp. 323–339, 2006.

[11] A. Xhelaj, M. Burlando, and G. Solari, "A general-purpose analytical model for reconstructing the thunderstorm outflows of travelling downbursts immersed in abl flows," *Journal of Wind Engineering and Industrial Aerodynamics*, vol. 207, p. 104373, 2020.

[12] T. Rajkumar, C. Aragon, J. Bardina, and R. Britten, "Prediction of aerodynamic coefficients for wind tunnel data using a genetic algorithm optimized neural network," tech. rep., NASA Ames Research Center, 2003.

[13] X. Liang, X. Gao, T. Gu, and X. Jia, "Aerodynamic drag coefficient analysis of heavy-duty vehicle platoons: A hybrid approach integrating wind tunnel experiments and cfd simulations," *Energies*, vol. 17, no. 24, p. 6383, 2024.

[14] F. Zhang, P. Hu, Y. Han, C. Cai, D. He, and F. Chen, "Dynamic response analysis of moving trains passing through the stationary thunderstorm downburst wind," *International Journal of Structural Stability and Dynamics*, vol. 25, 06 2024.

[15] A. Brandt, B. Jacobson, and S. Sebben, "High-speed driving stability of road vehicles under crosswinds: An aerodynamic and vehicle dynamic parametric sensitivity analysis," *Vehicle System Dynamics*, vol. 60, no. 1, pp. 1–24, 2021.

[16] Z. Zhang, J. Li, and G. Wencui, "Combined simulation of heavy truck stability under sudden and discontinuous direction change of crosswind with computational fluid dynamics and multi-body system vehicle dynamics software," *Advances in Mechanical Engineering*, vol. 10, p. 168781401878636, 07 2018.

[17] T. Tunay, L. Drugge, and C. O'Reilly, "The effects of different drivers' steering inputs on the response of heavy ground vehicles to crosswind disturbances," *Applied Sciences*, vol. 14, p. 270, 12 2023.

[18] C. J. Nash and D. J. Cole, "Identification and validation of a driver steering control model incorporating human sensory dynamics," *Vehicle System Dynamics*, vol. 58, no. 1, pp. 1–23, 2019.

[19] D. D. Salvucci and R. Gray, "A two-point visual control model of steering," *Perception*, vol. 33, no. 10, pp. 1233–1248, 2004.

[20] Y. Maruyama, "Driving simulator experiment on the moving stability of an automobile under strong crosswind," *Journal of Wind Engineering and Industrial Aerodynamics*, vol. 94, pp. 191–205, 04 2006.

[21] Politecnico di Milano, "Wind tunnel facility, gvpm - galleria del vento politecnico di milano," 2026.

[22] A. I. Heft, T. Indinger, and N. A. Adams, "Introduction of a new realistic generic car model for aerodynamic investigations," in *SAE 2012 World Congress & Exhibition*, (Detroit, MI, United States), SAE International, 2012.

[23] S. Mack, T. Indinger, N. A. Adams, and P. Unterlechner, "The ground simulation upgrade of the large wind tunnel at the technische universität münchen," in *SAE 2012 World Congress & Exhibition*, (Detroit, MI, United States), SAE International, 2012.

[24] J. Wojciak, P. Theissen, N. A. Adams, T. Indinger, and R. Demuth, "Investigation of unsteady vehicle aerodynamics under time-dependent flow conditions," in *29th AIAA Applied Aerodynamics Conference*, (Honolulu, HI, United States), American Institute of Aeronautics and Astronautics, 2011.

[25] A. I. Heft, T. Indinger, and N. A. Adams, "Experimental and numerical investigation of the drivaer model," in *ASME 2012 Fluids Engineering Division Summer Meeting, Volume 1: Symposia, Parts A and B*, (Rio Grande, Puerto Rico, USA), pp. 41–51, American Society of Mechanical Engineers, 2012.

[26] P. Gazzara, "Road vehicles' safety under crosswind using numerical dynamic simulations," master's thesis, Politecnico di Milano, Milan, Italy, 2024.

[27] M. S. Mat Ali, J. Jalasabri, A. M. Sood, S. Mansor, H. Shaharuddin, and S. Muhamad, "Wind noise from a-pillar and side view mirror of a realistic generic car model, drivaer," *International Journal of Vehicle Noise and Vibration*, vol. 14, no. 1, pp. 38–61, 2018.

[28] D. C. Forbes, G. J. Page, M. A. Passmore, and A. P. Gaylard, "A fully coupled, 6 degree-of-freedom, aerodynamic and vehicle handling crosswind simulation using the drivaer model," *SAE International Journal of Passenger Cars – Mechanical Systems*, vol. 9, no. 2, pp. 710–722, 2016.

[29] C. Strangfeld, D. Wieser, H.-J. Schmidt, R. Woszidlo, C. Nayeri, and C. Paschereit, "Experimental study of baseline flow characteristics for the realistic car model drivaer," in *SAE 2013 World Congress & Exhibition*, (Detroit, MI, United States), SAE International, 2013.

[30] F. Cheli, R. Corradi, E. Sabbioni, and G. Tomasini, "Wind tunnel tests on heavy road vehicles: Cross wind-induced loads—part 1," *Journal of Wind Engineering and Industrial Aerodynamics*, vol. 99, no. 10, pp. 1000–1010, 2011.

[31] F. Cheli, F. Ripamonti, E. Sabbioni, and G. Tomasini, "Wind tunnel tests on

heavy road vehicles: Cross wind induced loads—part 2," *Journal of Wind Engineering and Industrial Aerodynamics*, vol. 99, no. 10, pp. 1011–1024, 2011.

[32] M. Sterling, A. D. Quinn, D. M. Hargreaves, F. Cheli, E. Sabbioni, G. Tomasini, D. Delaunay, C. J. Baker, and H. Morvan, "A comparison of different methods to evaluate the wind-induced forces on a high-sided lorry," *Journal of Wind Engineering and Industrial Aerodynamics*, vol. 98, no. 1, pp. 10–20, 2010.

[33] J. Setiawan, M. Safarudin, and A. Singh, "Modeling, simulation and validation of 14 dof full vehicle model," in *Proceedings of the International Conference on Instrumentation, Communications, Information Technology, and Biomedical Engineering (ICICI-BME)*, pp. 1–6, 2009.

[34] H. B. Pacejka and I. J. M. Besselink, "Magic formula tyre model with transient properties," *Vehicle System Dynamics*, vol. 27, no. sup001, pp. 234–249, 1997.

[35] I. L. Pardo, "A co-simulation model for analysing the stability of road vehicles under downburst wind conditions," Master's thesis, Politecnico di Milano, 2025.

[36] Commissione di studio per le norme relative ai materiali stradali e costruzione e manutenzione delle strade, "Norme funzionali e geometriche per la costruzione delle strade," 2001.

[37] VI-Grade GmbH, "Vi-grade – real-time simulation software and professional driving simulators," 2026.

[38] Politecnico di Milano, "Drismi driving simulator facility presentation," 2026.

[39] A. Xhelaj and M. Burlando, "Application of metaheuristic optimization algorithms to evaluate the geometric and kinematic parameters of downbursts," *Advances in Engineering Software*, vol. 173, p. 103203, 2022.

[40] A. R. Prakash, "Evaluation of heavy-vehicle driver response to cross-wind using a dynamic driving simulator," Master's thesis, Politecnico di Milano, 2021.

[41] World Meteorological Organization, "The beaufort scale of wind force: Technical and operational aspects," technical report, World Meteorological Organization, Commission for Maritime Meteorology, Geneva, Switzerland, 1970.

07.
Appendix

This Appendix provides the numerical results of the sensitivity analysis described in Chapter 5.

- Figure 1 - Saloon Car
- Figure 2 - Small lorry Empty configurations
- Figure 3 - Small lorry Laden configurations

In these tables a colour map was applied, red cells indicating the more critical cases, while values in green cells tend to stay far from the dangerous zones.

Vehicle type:	Saloon car	Wind angle (degrees)				vehicle speed: 100 km/h														
Risk index:	Lane deviation (m)	0	10	20	30	40	50	60	70	80	90	100	110	120	130	140	150	160	170	180
Wind velocity (m/s)	15	0.695	0.645	0.582	0.598	0.572	0.575	0.701	0.605	0.57	0.779	0.782	0.789	0.795	0.776	0.733	0.695	1.046	0.912	0.746
	20	0.705	0.625	0.61	0.571	0.593	0.574	0.712	0.685	0.563	0.916	0.897	0.889	0.949	0.889	0.783	0.803	1.137	0.896	1.028
	25	0.726	0.615	0.641	0.594	0.595	0.59	0.7	0.774	0.64	1.071	1.017	0.988	1.112	1.014	0.874	0.968	1.236	0.911	1.275
	30	0.774	0.63	0.658	0.642	0.599	0.638	0.673	0.865	0.719	1.24	1.111	1.057	1.184	1.115	0.964	1.141	1.377	0.964	1.487
	35	0.847	0.641	0.694	0.692	0.667	0.692	0.771	0.96	0.821	1.395	1.144	1.163	1.223	1.248	1.005	1.298	1.457	1.011	1.654

Vehicle type:	Saloon car	Wind angle (degrees)																		
Risk index:	Lane invasion (%)	**0**	**10**	**20**	**30**	**40**	**50**	**60**	**70**	**80**	**90**	**100**	**110**	**120**	**130**	**140**	**150**	**160**	**170**	**180**
Wind velocity (m/s)	15	29.394	34.549	40.896	39.336	41.891	41.671	28.872	38.563	42.143	20.919	20.579	19.944	19.314	21.178	25.569	29.399	-6.232	7.386	24.26
	20	28.406	36.516	38.043	42.055	39.771	41.709	27.714	30.461	42.857	6.983	8.92	9.772	3.695	9.7	20.473	18.517	-15.454	9.019	-4.372
	25	26.28	37.605	34.885	39.715	39.594	40.122	28.926	21.453	35.034	-8.693	-3.264	-0.277	-12.87	-2.941	11.287	1.713	-25.447	7.531	-29.468
	30	21.431	36.047	33.17	34.834	39.157	35.181	31.715	12.149	27.042	-25.908	-12.76	-7.327	-20.187	-13.241	2.139	-15.816	-39.826	2.115	-50.989
	35	14.009	34.95	29.519	29.759	32.302	29.77	21.711	2.529	16.634	-41.579	-16.147	-18.046	-24.21	-26.658	-2.024	-31.813	-47.957	-2.606	-67.899

Vehicle type:	Saloon car	Wind angle (degrees)				front														
Risk index:	Load transfer ratio (%)	**0**	**10**	**20**	**30**	**40**	**50**	**60**	**70**	**80**	**90**	**100**	**110**	**120**	**130**	**140**	**150**	**160**	**170**	**180**
Wind velocity (m/s)	15	6.839	5.617	4.592	4.475	4.843	5.063	6.197	8.836	9.003	12.172	11.834	11.911	13.693	13.368	12.312	12.715	15.573	9.811	9.751
	20	7.753	6.293	4.851	4.658	4.819	5.465	7.114	10.396	11.049	14.423	14.097	14.519	16.923	16.124	14.85	16.496	18.324	12.208	12.459
	25	8.55	6.837	5.173	5.427	4.856	6.047	8.892	12.093	12.99	17.218	16.527	17.595	21.113	18.647	17.543	19.856	21.742	15.015	17.226
	30	10.099	8.637	5.541	6.824	4.886	6.703	10.783	13.682	14.967	20.457	18.464	20.912	24.518	21.526	20.218	24.326	25.174	19.039	22.246
	35	13.772	10.526	6.588	8.733	6.68	7.5	12.745	15.336	17.187	24.037	22.592	24.231	27.481	24.635	22.764	27.941	29.317	22.994	17.886

Vehicle type:	Saloon Car	Wind angle (degrees)				rear														
Risk index:	Load transfer ratio (%)	**0**	**10**	**20**	**30**	**40**	**50**	**60**	**70**	**80**	**90**	**100**	**110**	**120**	**130**	**140**	**150**	**160**	**170**	**180**
Wind velocity (m/s)	15	4.355	3.558	2.902	2.865	3.051	3.17	3.959	5.56	5.68	7.757	7.551	7.569	8.799	8.499	7.739	8.024	9.92	6.208	6.159
	20	5.004	3.952	3.072	2.967	3.035	3.406	4.429	6.58	7.022	9.219	9.069	9.384	10.917	10.41	9.527	10.654	11.822	7.75	7.893
	25	5.558	4.497	3.255	3.526	3.061	3.796	5.579	7.708	8.304	11.095	10.726	11.566	13.89	12.099	11.316	12.993	14.32	9.67	11.124
	30	6.978	5.859	3.643	4.535	3.188	4.206	6.816	8.764	9.603	13.281	12.166	13.908	16.411	14.209	13.153	16.256	16.818	12.449	14.755
	35	9.795	7.37	4.629	5.98	4.536	4.629	8.118	9.872	11.113	15.789	15.279	16.14	18.76	17.176	15.092	18.876	19.976	15.274	26.442

Figure 7.1: Sensitivity analysis results - Saloon Car

Vehicle type:	Empty Lorry	Wind angle (degrees)			vehicle speed: 100 km/h															
Risk index:	Lane deviation (m)	0	10	20	30	40	50	60	70	80	90	100	110	120	130	140	150	160	170	180
Wind velocity (m/s)	15	0.39	0.243	0.127	0.146	0.241	0.362	0.586	0.725	0.838	0.924	1.056	1.086	1.083	1.192	0.983	1.094	0.957	0.836	0.793
	20	0.573	0.358	0.166	0.14	0.278	0.428	0.739	0.912	1.101	1.083	1.138	1.168	1.098	1.25	1.172	2	2	0.964	0.955
	25	0.804	0.486	0.244	0.196	0.318	0.51	0.896	1.17	2	2	2	2	2	2	2	2	2	0.893	0.994
	30	1.099	0.686	0.379	0.328	0.36	0.613	0.996	2	2	2	2	2	2	2	2	2	2	2	2
	35	1.634	0.955	0.602	0.527	0.405	0.723	1.106	2	2	2	2	2	2	2	2	2	2	2	2
Vehicle type:	Empty Lorry	Wind angle (degrees)																		
Risk index:	Lane invasion (%)	0	10	20	30	40	50	60	70	80	90	100	110	120	130	140	150	160	170	180
Wind velocity (m/s)	15	37.534	61.132	79.728	76.601	61.388	42.074	6.189	-16.06	-34.096	-47.898	-68.961	-73.837	-73.245	-90.73	-57.323	-75.046	-53.18	-33.744	-26.81
	20	8.397	42.696	73.517	77.638	55.554	31.539	-18.201	-45.947	-76.203	-73.334	-82.146	-86.895	-75.721	-100.05	-87.469	-220	-220	-54.2	-52.831
	25	-28.704	22.246	61.038	68.569	49.197	18.324	-43.416	-87.27	-220	-220	-220	-220	-220	-220	-220	-220	-220	-42.806	-59.04
	30	-75.856	-9.795	39.421	47.442	42.393	1.999	-59.312	-220	-220	-220	-220	-220	-220	-220	-220	-220	-220	-220	-220
	35	-161.4	-52.727	3.609	15.727	35.127	-15.606	-76.919	-220	-220	-220	-220	-220	-220	-220	-220	-220	-220	-220	-220
Vehicle type:	Empty Lorry	Wind angle (degrees)					front													
Risk index:	Load transfer ratio (%)	0	10	20	30	40	50	60	70	80	90	100	110	120	130	140	150	160	170	180
Wind velocity (m/s)	15	23.104	14.45	8.02	9.617	15.385	21.956	34.686	44.652	49.959	53.047	75.961	76.089	76.338	84.021	62.231	72.324	71.673	51.988	45.188
	20	33.853	19.237	10.029	9.328	17.537	25.573	42.587	55.353	68.643	73.567	89.133	97.917	82.717	97.963	92.003	120	120	68.595	59.935
	25	47.362	26.587	14.432	12.371	19.796	30.685	50.774	79.589	120	120	120	120	120	120	120	120	120	89.754	85.275
	30	63.681	38.469	23.876	18.177	22.089	36.533	66.064	120	120	120	120	120	120	120	120	120	120	120	120
	35	97.656	55.429	39.55	26.026	24.505	42.402	84.717	120	120	120	120	120	120	120	120	120	120	120	120
Vehicle type:	Empty Lorry	Wind angle (degrees)					rear													
Risk index:	Load transfer ratio (%)	0	10	20	30	40	50	60	70	80	90	100	110	120	130	140	150	160	170	180
Wind velocity (m/s)	15	39.208	24.074	13.099	16.113	26.336	37.66	58.539	75.463	84.77	91.754	100.999	97.451	96.718	103.675	104.622	98.771	103.94	92.948	79.543
	20	55.12	32.054	16.227	15.76	30.142	44.672	71.948	97.205	98.813	101.926	97.94	101.435	102.456	102.279	108.463	120	120	99.503	106.558
	25	74.907	44.684	23.838	20.29	34.356	52.975	87.99	98.246	120	120	120	120	120	120	120	120	120	104.256	105.724
	30	100.459	60.522	39.969	30.379	39.008	62.506	100.808	120	120	120	120	120	120	120	120	120	120	120	120
	35	108.071	85.685	62.059	43.398	43.934	72.876	102.241	120	120	120	120	120	120	120	120	120	120	120	120

Figure 7.2: Sensitivity analysis results - Empty lorry

Vehicle type:	Laden Lorry	Wind angle (degrees)			vehicle speed: 100 km/h															
Risk index:	Lane deviation (m)	0	10	20	30	40	50	60	70	80	90	100	110	120	130	140	150	160	170	180
Wind velocity (m/s)	15	0.324	0.192	0.197	0.213	0.243	0.307	0.494	0.508	0.601	0.659	0.786	0.938	0.971	0.967	0.707	1.061	1.247	0.869	1.105
	20	0.429	0.273	0.2	0.215	0.251	0.37	0.61	0.633	0.691	0.827	1.05	1.245	1.309	1.162	0.954	1.442	1.344	0.988	1.461
	25	0.522	0.354	0.202	0.212	0.288	0.443	0.745	0.775	0.894	1.084	1.448	1.734	1.882	1.443	1.29	1.974	1.44	1.246	1.759
	30	0.731	0.473	0.304	0.206	0.329	0.524	0.898	0.934	1.167	1.457	2	2	2	2	1.869	2	2	1.748	2
	35	1.066	0.68	0.474	0.295	0.387	0.611	1.065	1.118	1.524	2	2	2	2	2	2	2	2	2	2
Vehicle type:	Laden Lorry	Wind angle (degrees)																		
Risk index:	Lane invasion (%)	0	10	20	30	40	50	60	70	80	90	100	110	120	130	140	150	160	170	180
Wind velocity (m/s)	15	48.105	69.349	68.472	65.892	61.189	50.831	20.937	18.786	3.9	-5.383	-25.714	-50.096	-55.379	-54.782	-13.197	-69.695	-99.495	-38.989	-76.841
	20	31.323	56.341	67.941	65.623	59.821	40.745	2.419	-1.359	-10.524	-32.27	-68.073	-99.21	-109.37	-85.929	-52.607	-130.68	-115.04	-58.06	-133.84
	25	16.535	43.332	67.604	66.135	53.98	29.128	-19.19	-24.068	-42.969	-73.5	-131.68	-177.51	-201.18	-130.91	-106.46	-215.8	-130.34	-99.342	-181.4
	30	-17.019	24.388	51.362	66.993	47.342	16.199	-43.638	-49.467	-86.763	-133.19	-220	-220	-220	-220	-199.01	-220	-220	-179.65	-220
	35	-70.482	-8.814	24.161	52.727	38.004	2.205	-70.455	-78.956	-143.88	-220	-220	-220	-220	-220	-220	-220	-220	-220	-220
Vehicle type:	Laden Lorry	Wind angle (degrees)						front												
Risk index:	Load transfer ratio (%)	0	10	20	30	40	50	60	70	80	90	100	110	120	130	140	150	160	170	180
Wind velocity (m/s)	15	11.615	6.947	5.028	5.483	8.812	12.99	19.606	24.584	25.317	26.442	33.833	36.467	36.991	35.874	31.477	33.974	37.851	29.135	32.046
	20	17.735	10.139	6.335	5.394	10.099	15.339	23.685	29.812	31.861	33.768	43.203	46.053	47.107	45.051	41.11	44.635	49.428	36.673	41.832
	25	23.01	13.651	8.287	6.496	11.549	17.885	28.164	35.519	39.51	42.219	54.317	57.436	60.065	56.298	50.948	58.415	60.124	45.528	52.89
	30	29.659	20.108	11.177	10.204	13.094	20.603	32.959	41.744	48.016	52.761	66.253	71.535	79.43	68.119	65.635	85.612	83.37	58.931	72.455
	35	37.88	28.337	17.186	15.856	14.732	23.446	38.001	48.492	57.067	68.519	75.722	84.183	120	120	80.31	120	120	80.703	120
Vehicle type:	Laden Lorry	Wind angle (degrees)						rear												
Risk index:	Load transfer ratio (%)	0	10	20	30	40	50	60	70	80	90	100	110	120	130	140	150	160	170	180
Wind velocity (m/s)	15	13.256	7.914	5.727	6.244	10.021	14.771	22.296	27.953	28.828	30.092	38.482	41.537	42.08	40.848	35.878	38.734	43.022	33.117	36.44
	20	20.258	11.564	7.22	6.143	11.488	17.446	26.956	33.901	36.276	38.433	49.008	52.185	53.284	51.149	46.666	50.948	56.014	41.69	47.5
	25	26.322	15.54	9.437	7.419	13.135	20.345	32.054	40.392	44.944	47.916	60.379	63.619	66.183	62.251	57.485	64.913	67.14	52.01	59.825
	30	33.968	22.912	12.828	11.635	14.89	23.439	37.508	47.472	54.16	58.734	72.997	78.365	86.781	75.378	72.248	94.149	92.006	65.737	79.957
	35	43.442	32.338	19.717	18.089	16.75	26.675	43.236	54.916	63.491	75.145	83.833	92.099	120	120	88.668	120	120	89.145	120

Figure 7.3: Sensitivity analysis results - Laden lorry